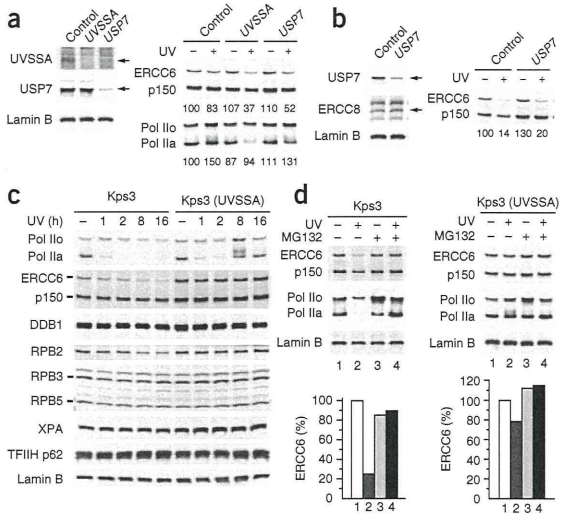

Figure 4 Degradation of ERCC6 in parental Kps3 cells, UVSSA-corrected Kps3 cells and normal cells transfected with *USP7* siRNA after UV irradiation. (**a**) UV-induced degradation of ERCC6 and RNA Pol IIo in normal cells transfected with control siRNA or siRNA targeting *UVSSA* or *USP7*. Knockdown of *UVSSA* and *USP7* was confirmed by protein blotting of cell lysates using the indicated antibodies. Normal cells transfected with each siRNA were irradiated with 10 J/m^2 of UV or not irradiated and were incubated for 16 h. Samples lysed with SDS gel-loading buffer were then analyzed by protein blotting with antibody to ERCC6. Numbers below the blots indicate the amounts of ERCC6 (upper) and RNA Pol IIo (lower) relative to their amounts in non-irradiated normal cells transfected with control siRNA. (**b**) UV-induced degradation of ERCC6 in Kps3 cells transfected with control siRNA or with siRNA targeting *UVSSA* or *USP7*. Knockdown by siRNA and protein blotting were performed as in **c**, except for an 8-h incubation after UV irradiation. Numbers below the blot indicate the amount of ERCC6 relative to the amount in non-irradiated Kps3 cells transfected with control siRNA. (**c**) Parental Kps3 cells and UVSSA-corrected Kps3 cells were irradiated with 10 J/m^2 of UV and incubated for the indicated times. Samples lysed with SDS gel-loading buffer were analyzed by protein blotting using the indicated antibodies. DDB1, UV-damaged DNA binding protein 1; RPB2, second largest subunit of RNA Pol II; RPB3, third largest subunit of RNA Pol II; RPB5, fifth largest subunit of RNA Pol II; XPA, xeroderma pigmentosum group A protein. Only RPB2 was decreased to some extent in UV-irradiated Kps3 cells. (**d**) Inhibition of the degradation of ERCC6 and the reappearance of RNA Pol IIa after UV irradiation in Kps3 cells in the presence of MG132. Parental Kps3 cells and UVSSA-corrected Kps3 cells were either irradiated with 10 J/m^2 of UV or not irradiated and were incubated for 8 h in the presence (10 μM) or absence of the proteasome inhibitor MG132. Samples lysed with SDS gel-loading buffer were analyzed by protein blotting using the indicated antibodies. Histograms indicate the amount of ERCC6 relative to the amount in non-irradiated cells in the absence of MG132.

that UVSSA has an important role in stabilizing ERCC6 in TCR. In addition, ERCC6 was degraded in the *USP7* siRNA–treated cells, as in the *UVSSA* siRNA–treated cells, but not in control siRNA–treated cells (**Fig. 4a**). Kps3 cells that lack *UVSSA* were then treated with *USP7* siRNA. No significant difference in UV-induced degradation of ERCC6 was detected between control siRNA– and *USP7* siRNA–treated Kps3 cells (**Fig. 4b**). These results indicate that UVSSA and USP7 cooperate to protect ERCC6 from UV-induced degradation in TCR.

When the Kps3 cells were UV irradiated in the presence of the proteasome inhibitor MG132, the reduction in ERCC6 levels after UV irradiation was suppressed, and RNA Pol IIa reappeared 16 h after UV irradiation (**Fig. 4d**). These results suggest that, in UV-irradiated Kps3 cells, ERCC6 is ubiquitinated and degraded by the ubiquitin-proteasome pathway, and the recovery of RNA Pol IIa is blocked, leading to the inhibition of UV-RRS.

The amount of RNA Pol IIo decreased in parental Kps3 cells (**Fig. 4c**) and in *UVSSA* siRNA–treated normal cells (**Fig. 4a**), although the decrease in RNA Pol IIo was not significant compared with that of ERCC6. RNA Pol IIo levels did not decrease in the UVSSA-corrected Kps3 cells and in control siRNA–treated cells (**Fig. 4a**,**c**). In the *USP7* siRNA–treated cells, the amount of RNA Pol IIo slightly decreased after UV irradiation when compared to the amount in control siRNA–treated cells (**Fig. 4a**). Taken together, these results suggest that UVSSA and USP7 are involved in the stabilization of RNA Pol IIo, but the effect might be indirect.

The affected individuals with the UV^{S}S, UV^{S}1KO and UV^{S}1VI, had homozygous mutations in the *ERCC6* and *ERCC8* genes, respectively[5,6]. This prompted us to examine whether some individuals with Cockayne syndrome features and TCR deficiency have mutations in the *UVSSA* gene. We sequenced the ORF of *UVSSA* in three TCR-deficient Cockayne syndrome cell lines (CS7099, CS6864 and CS2760) that have no mutations in the *ERCC6* and *ERCC8* genes. We found only SNPs in *UVSSA* in these cells (**Supplementary Fig. 7**), suggesting that there are some other gene(s) involved in the Cockayne syndrome phenotype beyond *ERCC6* and *ERCC8*. To exclude the possibility that some individuals with Cockayne syndrome have mutations in *UVSSA*, it is necessary to sequence the *UVSSA* ORF in many other TCR-deficient subjects with Cockayne syndrome.

It has been reported that CS-A and CS-B cells are hypersensitive to treatment with hydrogen peroxide and potassium bromate, specific inducers of oxidative DNA damage, and are deficient in the repair of oxidative DNA damage, whereas Kps3 (UV^{S}SA) and UV^{S}S1VI (UV^{S}S/CS-A) cells are not hypersensitive to oxidative DNA damage[6,21,22]. It has also been reported that transcription by RNA Pol II was reduced in the extracts of CS-A and CS-B cells compared to transcription levels in normal cells[23,24]. Nuclear extracts of CS-B cells failed to transcribe human rDNA, whereas those of CS-B cells expressing wild-type ERCC6 showed high transcriptional activity of RNA Pol I (ref. 25). Of note, RNA Pol I transcription was proficient in UV^{S}1KO (UV^{S}S/CS-B) cells[26]. Taken together, these results suggest that marked differences in the pathological phenotypes between Cockayne syndrome and UV^{S}S are caused by differences in transcription and/or in the repair of oxidative DNA damage in affected individuals.

We also determined that ERCC6 was ubiquitinated and degraded by the ubiquitin-proteasome pathway after UV irradiation in Kps3 cells (**Fig. 4c**,**d**). It has been reported that ERCC6 is required for the resumption of transcription after UV irradiation and for the recruitment of RNA Pol II and other transcription factors at the promoter in UV-irradiated cells[27]. It is therefore suggested that the ubiquitination and degradation of ERCC6 in the absence of UVSSA prevents recovery of RNA Pol IIa after UV irradiation and, consequently, blocks UV-RRS (**Supplementary Fig. 8**). Kps3 cells are deficient in the removal of UV damage on transcribed DNA strands[28], indicating that UVSSA is also required for excision of DNA damage in TCR (**Supplementary Fig. 8**).

It is not yet clear which E3 ligase is involved in the ubiquitination of ERCC6 in TCR. It would be interesting to examine whether ERCC6 is ubiquitinated by ERCC8 (ref. 29), BRCA1-BARD1 (ref. 30) or the p44 subunit of TFIIH[31]. UVSSA may negatively regulate E3 ligase activities. Alternatively or simultaneously, it may positively regulate

the deubiquitinase activity of USP7 to stabilize ERCC6 in TCR. We conclude that the UVSSA-USP7 complex has an important role in TCR, whereby it controls the steady-state levels of ERCC6.

METHODS

Methods and any associated references are available in the online version of the paper at http://www.nature.com/naturegenetics/.

Note: Supplementary information is available on the Nature Genetics website.

ACKNOWLEDGMENTS

We thank Y. Iwamoto and I. Kuraoka for their help in DNA sequencing and microcell-mediated chromosome transfer and M. Hoshi for her help in establishing Flp-In cells and performing immunoprecipitation. We also thank M. Yamaizumi (Kumamoto University Medical School) and N.G. Jaspers (Erasmus Medical Centre) for providing Kps3 cells and TA-24 cells, respectively. We thank G. Spivak for critical reading of the manuscript. This work was supported by a Grant-in-Aid for Scientific Research on Innovative Areas from the Ministry of Education, Culture, Sports, Science and Technology (MEXT) of Japan and by Health and Labor Sciences Research Grants for Research on Intractable Diseases (to K.T.). Part of this work was carried out under the Cooperative Research Project Program of the Institute of Development, Aging and Cancer (IDAC) at Tohoku University.

AUTHOR CONTRIBUTIONS

X.Z., K.H., M.S. and K.T. conceived the experiments. K.T. and H.T. established the cell lines. X.Z., K.H. and C.I. performed microcell-mediated chromosome transfer. A.U., K.H. and M.H. performed CGH array analysis. X.Z., M.S. and S.K. performed biochemical analysis. E.G.N. diagnosed Cockayne syndrome patients. K.T., X.Z., K.H., M.S., M.H., T.N. and A.Y. analyzed the data. K.T., X.Z., M.S. and K.H. wrote the manuscript.

COMPETING FINANCIAL INTERESTS

The authors declare no competing financial interests.

Published online at http://www.nature.com/naturegenetics/.
Reprints and permissions information is available online at http://www.nature.com/reprints/index.html.

1. Hanawalt, P.C. & Spivak, G. Transcription-coupled DNA repair: two decades of progress and surprises. *Nat. Rev. Mol. Cell Biol.* **9**, 958–970 (2008).
2. Fousteri, M. & Mullenders, L.H. Transcription-coupled nucleotide excision repair in mammalian cells: molecular mechanisms and biological effects. *Cell Res.* **18**, 73–84 (2008).
3. Spivak, G. UV-sensitive syndrome. *Mutat. Res.* **577**, 162–169 (2005).
4. Itoh, T., Ono, T. & Yamaizumi, M. A new UV-sensitive syndrome not belonging to any complementation groups of xeroderma pigmentosum or Cockayne syndrome: siblings showing biochemical characteristics of Cockayne syndrome without typical clinical manifestations. *Mutat. Res.* **314**, 233–248 (1994).
5. Horibata, K. *et al.* Complete absence of Cockayne syndrome group B gene product gives rise to UV-sensitive syndrome but not Cockayne syndrome. *Proc. Natl. Acad. Sci. USA* **101**, 15410–15415 (2004).
6. Nardo, T. *et al.* A UV-sensitive syndrome patient with a specific *CSA* mutation reveals separable roles for CSA in response to UV and oxidative DNA damage. *Proc. Natl. Acad. Sci. USA* **106**, 6209–6214 (2009).
7. Nagase, T., Kikuno, R., Ishikawa, K., Hirosawa, M. & Ohara, O. Prediction of the coding sequences of unidentified human genes. XVII. The complete sequences of 100 new cDNA clones from brain which code for large proteins *in vitro*. *DNA Res.* **7**, 143–150 (2000).
8. Nicholson, B. & Suresh Kumar, K.G. The multifaceted roles of USP7: new therapeutic opportunities. *Cell Biochem. Biophys.* **60**, 61–68 (2011).
9. Sanford, J.A. & Stubblefield, E. General protocol for microcell-mediated chromosome transfer. *Somat. Cell Mol. Genet.* **13**, 279–284 (1987).
10. Abe, K. *et al.* Contribution of Asian mouse subspecies *Mus musculus molossinus* to genomic constitution of strain C57BL/6J, as defined by BAC-end sequence-SNP analysis. *Genome Res.* **14**, 2439–2447 (2004).
11. Itoh, T., Linn, S., Ono, T. & Yamaizumi, M. Reinvestigation of the classification of five cell strains of xeroderma pigmentosum group E with reclassification of three of them. *J. Invest. Dermatol.* **114**, 1022–1029 (2000).
12. Strausberg, R.L. *et al.* Generation and initial analysis of more than 15,000 full-length human and mouse cDNA sequences. *Proc. Natl. Acad. Sci. USA* **99**, 16899–16903 (2002).
13. Meinhart, A. & Cramer, P. Recognition of RNA polymerase II carboxy-terminal domain by 3′-RNA-processing factors. *Nature* **430**, 223–226 (2004).
14. Steinmetz, E.J., Conrad, N.K., Brow, D.A. & Corden, J.L. RNA-binding protein Nrd1 directs poly(A)-independent 3′-end formation of RNA polymerase II transcripts. *Nature* **413**, 327–331 (2001).
15. Khoronenkova, S.V., Dianova, I.I., Parsons, J.L. & Dianov, G.L. USP7/HAUSP stimulates repair of oxidative DNA lesions. *Nucleic Acids Res.* **39**, 2604–2609 (2011).
16. Schwertman, P. *et al.* UV-sensitive syndrome protein UVSSA recruits USP7 to regulate transcription-coupled repair. *Nat. Genet.* published online (1 April 2012); doi:10.1038/ng.2230.
17. Kamiuchi, S. *et al.* Translocation of Cockayne syndrome group A protein to the nuclear matrix: possible relevance to transcription-coupled DNA repair. *Proc. Natl. Acad. Sci. USA* **99**, 201–206 (2002).
18. Fousteri, M., Vermeulen, W., vanZeeland, A.A. & Mullenders, L.H. Cockayne syndrome A and B proteins differentially regulate recruitment of chromatin remodeling and repair factors to stalled RNA polymerase II *in vivo*. *Mol. Cell* **23**, 471–482 (2006).
19. Saijo, M. *et al.* Functional TFIIH is required for UV-induced translocation of CSA to the nuclear matrix. *Mol. Cell. Biol.* **27**, 2538–2547 (2007).
20. Rockx, D.A. *et al.* UV-induced inhibition of transcription involves repression of transcription initiation and phosphorylation of RNA polymerase II. *Proc. Natl. Acad. Sci. USA* **97**, 10503–10508 (2000).
21. Spivak, G. & Hanawalt, P.C. Host cell reactivation of plasmids containing oxidative DNA lesions is defective in Cockayne syndrome but normal in UV-sensitive syndrome fibroblasts. *DNA Repair (Amst.)* **5**, 13–22 (2006).
22. D'Errico, M. *et al.* The role of CSA in the response to oxidative DNA damage in human cells. *Oncogene* **26**, 4336–4343 (2007).
23. Selby, C.P. & Sancar, A. Cockayne syndrome group B protein enhances elongation by RNA polymerase II. *Proc. Natl. Acad. Sci. USA* **94**, 11205–11209 (1997).
24. Dianov, G.L., Houle, J.F., Iyer, N., Bohr, V.A. & Friedberg, E.C. Reduced RNA polymerase II transcription in extracts of cockayne syndrome and xeroderma pigmentosum/Cockayne syndrome cells. *Nucleic Acids Res.* **25**, 3636–3642 (1997).
25. Bradsher, J. *et al.* CSB is a component of RNA pol I transcription. *Mol. Cell* **10**, 819–829 (2002).
26. Lebedev, A., Scharffetter-Kochanek, K. & Iben, S. Truncated Cockayne syndrome B protein represses elongation by RNA polymerase I. *J. Mol. Biol.* **382**, 266–274 (2008).
27. Proietti-De-Santis, L., Drane, P. & Egly, J.M. Cockayne syndrome B protein regulates the transcriptional program after UV irradiation. *EMBO J.* **25**, 1915–1923 (2006).
28. Spivak, G. *et al.* Ultraviolet-sensitive syndrome cells are defective in transcription-coupled repair of cyclobutane pyrimidine dimers. *DNA Repair (Amst.)* **1**, 629–643 (2002).
29. Groisman, R. *et al.* CSA-dependent degradation of CSB by the ubiquitin-proteasome pathway establishes a link between complementation factors of the Cockayne syndrome. *Genes Dev.* **20**, 1429–1434 (2006).
30. Wei, L. *et al.* BRCA1 contributes to transcription-coupled repair of DNA damage through polyubiquitylation and degradation of Cockayne syndrome B protein. *Cancer Sci.* **102**, 1840–1847 (2011).
31. Takagi, Y. *et al.* Ubiquitin ligase activity of TFIIH and the transcriptional response to DNA damage. *Mol. Cell* **18**, 237–243 (2005).
32. Horibata, K. *et al.* Mutant Cockayne syndrome group B protein inhibits repair of DNA topoisomerase I–DNA covalent complex. *Genes Cells* **16**, 101–114 (2011).

ONLINE METHODS

Cell lines. Kps3, XP24KO and TA-24 cells belong to UV^{S}S-A and were immortalized by simian virus 40 large T antigen and hTERT. FS3 and WI38VA13 are normal human cells. Mouse A9 cells were used as donors in microcell-mediated chromosome transfer. All cell lines used were cultured in DMEM containing 10% FCS, penicillin and streptomycin at 37 °C under 5% CO_2.

UV survival. Cells were inoculated in 10-cm dishes at a density of 1,000–2,000 cells per dish. After 6 h, cells were washed with PBS and irradiated with UV at 0, 5 and 10 J/m^2. Cells were then incubated for 1–2 weeks. Resulting colonies were fixed with 3.7% formaldehyde and stained with 0.1% crystal violet and were counted using a binocular microscope.

Microcell-mediated chromosome transfer. Donor A9 cells were plated onto 25-cm^2 flasks in DMEM supplemented with 10% FCS. After 1–3 d (when cells were 80% confluent), the culture medium was changed to DMEM supplemented with 20% FCS and 50 ng/ml colcemid (Sigma). After 48 h of incubation, flasks were centrifuged at 12,000*g* for 1 h in the presence of 10 μg/ml cytochalasin B (Sigma) for enucleation. The microcell pellets were resuspended in serum-free DMEM and sequentially filtered through polycarbonate membranes with pores of 8, 5 and 3 μm in diameter. Purified microcells, which were irradiated with 10 Gy of γ-irradiation in some experiments, were plated onto a monolayer of recipient Kps3 cells in a 6-cm dish with serum-free DMEM containing 50 μg/ml phytohemagglutinin P (Sigma). After 30 min of incubation, the microcells were fused with recipient cells by treating the cells with 50% polyethylene glycol 1000 (Nakarai) for 1 min. After fusion, cells were grown for 24 h in DMEM supplemented with10% FCS. Then, cells were replated onto six 10-cm dishes and incubated for 24 h. Cells were irradiated with 10 J/m^2 of UV light. Surviving cells were collected and replated onto six 10-cm dishes and allowed to grow for 7 d. Cells were then irradiated with 10 J/m^2 of UV light. In total, cells were irradiated six times at 7-d intervals. As a negative control, Kps3 cells fused in the absence of microcells were UV irradiated in the same manner.

Comparative genomic hybridization array analysis. The regions of segmented mouse chromosomes transferred to Kps3 cells were analyzed using a Mouse Genome CGH 244A Oligo Microarray Kit with SurePrint Technology (Agilent Technologies), according to the manufacturer's instructions with some modifications. In brief, genomic DNA derived from the 15A-7, KAGB2-4, KAGA2-6 and KAB1-14 clones was compared with genomic DNA from parental Kps3 cells on the arrays. Genomic DNA was extracted by Qiagen Gentra Puregene core Kit A. After digestion with AluI and RsaI, the genomic DNA derived from Kps3 cells was labeled with Cy3, and the genomic DNA from the 15A-7, KAGB2-4, KAGA2-6 and KAB1-14 clones was labeled with Cy5, using a Genomic DNA Enzymatic Labeling Kit (Agilent Technologies). To prevent nonspecific hybridization of human genomic DNA on the array, 50 μg of human Cot-1 DNA (Invitrogen) and 5 μg of mouse Cot-1 DNA (Invitrogen) were mixed and subjected to prehybridization. After hybridization with the labeled genomic DNA, arrays were washed and scanned with GenePix4000B. Scanned data were analyzed by Feature Extraction Software version 9.5 and DNA Analytics version 4.0 (both from Agilent Technologies).

Transfection of mouse BACs. Mouse BAC clones were amplified in *Escherichia coli* cultured in LB medium containing chloramphenicol (25 μg/ml). BAC DNA was prepared with a Midiprep Kit (Qiagen), following the manufacturer's instructions. BAC DNA (20 μg) was cotransfected with 0.6 μg of pSV2neo into recipient Kps3 cells grown on a 10-cm tissue culture dish, and cells were selected with medium containing G418 (400 μg/ml) and irradiated with 10 J/m^2 of UV twice at 4–d intervals to examine whether the BAC-transfected Kps3 clones acquired a normal level of UV resistance.

Recovery of RNA synthesis after UV irradiation. To measure RNA synthesis after UV irradiation, two sets of cells were seeded into 6-well culture plates (1×10^6 cells/well). One set was used for counting cells and the other for measuring RNA synthesis. After 6 h of incubation, cells were washed with PBS and treated with UV at 10 J/m^2. After 2, 4, 8 and 24 h of incubation, the number of cells in one set was counted. The other set of cells was washed with PBS and incubated in DMEM containing 370 kBq/ml of [^{3}H]-uridine for 30 min to quantify RNA synthesis. Labeling was terminated by the addition of sodium azide to a final concentration of 200 μg/ml. Cells were washed twice with PBS containing 200 μg/ml sodium azide and lysed in 0.8% SDS for 30 min at room temperature. An equal volume of 10% trichloroacetic acid containing 0.1 M sodium pyrophosphate was then added to the lysates, and these were incubated on ice for 1 h. Acid-insoluble materials were collected on GF-C glass microfiber filters (Whatman), and radioactivity was measured with an LS 6500 liquid scintillation counter (Beckman Coulter). Total radioactivity was divided by the number of cells to obtain single-cell radioactivity. The ratio (as a percentage) of the radioactivity of individual UV-irradiated cells to that of non-irradiated cells was considered as a measure of the recovery of RNA synthesis after UV irradiation (UV-RRS).

Immunoprecipitation. Cells stably expressing a Flag- and HA-tagged protein were lysed with MNase buffer (20 mM Tris-HCl, pH 7.5, 100 mM KCl, 300 mM sucrose, 2 mM $MgCl_2$, 0.1% Triton X-100, 1 mM $CaCl_2$, 1 mM DTT and complete protease inhibitor cocktail (Roche)) at 4 °C for 10 min. Lysates were centrifuged at 3,800*g* for 5 min. Supernatant was used as the soluble fraction. The pellet was washed once with MNase buffer and incubated with 30 U/ml of micrococcal nuclease (Takara) in MNase buffer at 25 °C for 30 min. The reaction was terminated by adding EDTA to a 5 mM final concentration and centrifuged at 3,800*g* for 5 min at 4 °C. The pellet was washed with MNase buffer. Supernatants were combined and used as the solubilized chromatin fraction. Tagged protein was affinity purified from the soluble and solubilized chromatin fractions with anti-FLAG M2 antibody-conjugated agarose (Sigma) followed by anti-HA agarose (Sigma).

Knockdown experiments. siRNA (Thermo Scientific) was transfected into target cells with RNAiMAX (Invitrogen), according to the manufacturer's instructions. At 24 h after the first transfection, a second transfection was performed. Cells were allowed to grow for another 36 h before experiments were carried out.

Quantitative RT-PCR. cDNA was synthesized from fresh total RNA using a Quantitative Reverse Transcription kit (Qiagen), following the manufacturer's instructions. RT-PCR samples were prepared with TaqMan gene expression master mix (Applied Biosystems), according to the manufacturer's instructions. RT-PCR was carried out using the 7300 Real-Time PCR system (Applied Biosystems), under the following conditions: 10 s at 95 °C, 10 s at 60 °C and 20 s at 72 °C for 25 cycles. Probe sets were ordered from Applied Biosystems.

UV-induced translocation of ERCC8 to the nuclear matrix using a cell-free system. UV-induced translocation of ERCC8 in the cell-free system was examined as described previously[19]. Parental Kps3 cells and UVSSA-corrected Kps3 cells were irradiated with 20 J/m^2 of UV and incubated for 1 h and then treated with CSK-Triton buffer (10 mM PIPES, pH 6.8, 100 mM NaCl, 300 mM sucrose, 3 mM $MgCl_2$, 0.5% Triton X-100, 1 mM DTT, 1 mM EGTA and Complete protease inhibitor cocktail (Roche)) to prepare the insoluble (CSK-ppt) fractions. The soluble fractions (CSK-sup) were prepared from CS3BE (CS-A) cells stably expressing Flag- and HA-tagged ERCC8 by treatment with CSK-Triton buffer. The CSK-sup fraction containing HA-tagged ERCC8 was incubated with the CSK-ppt fraction and then treated with DNase I. The ERCC8 retained in the DNase I–insoluble fractions was detected by immunoblotting with antibody to HA.

Antibodies. The antibodies employed were to ERCC8 (W-16, Santa Cruz Biotechnology), ERCC6 (E-18, Santa Cruz Biotechnology), RNA Pol II (N-20 and A-10, Santa Cruz Biotechnology), KIAA1530 (106751, GeneTex) and HA (3F10, Roche).

doi:10.1038/ng.2228

Sato et al. BMC Musculoskeletal Disorders 2012, 13:51
http://www.biomedcentral.com/1471-2474/13/51

BMC Musculoskeletal Disorders

RESEARCH ARTICLE Open Access

Human telomerase reverse transcriptase and glucose-regulated protein 78 increase the life span of articular chondrocytes and their repair potential

Masato Sato[1*], Kazuo Shin-ya[2], Jeong Ik Lee[3], Miya Ishihara[4], Toshihiro Nagai[1], Nagatoshi Kaneshiro[1], Genya Mitani[1], Hidetoshi Tahara[5] and Joji Mochida[1]

Abstract

Background: Like all mammalian cells, normal adult chondrocytes have a limited replicative life span, which decreases with age. To facilitate the therapeutic use of chondrocytes from older donors, a method is needed to prolong their life span.

Methods: We transfected chondrocytes with hTERT or GRP78 and cultured them in a 3-dimensional atelocollagen honeycomb-shaped scaffold with a membrane seal. Then, we measured the amount of nuclear DNA and glycosaminoglycans (GAGs) and the expression level of type II collagen as markers of cell proliferation and extracellular matrix formation, respectively, in these cultures. In addition, we allografted this tissue-engineered cartilage into osteochondral defects in old rabbits to assess their repair activity in vivo.

Results: Our results showed different degrees of differentiation in terms of GAG content between chondrocytes from old and young rabbits. Chondrocytes that were cotransfected with hTERT and GRP78 showed higher cellular proliferation and expression of type II collagen than those of nontransfected chondrocytes, regardless of the age of the cartilage donor. In addition, the in vitro growth rates of hTERT- or GRP78-transfected chondrocytes were higher than those of nontransfected chondrocytes, regardless of donor age. In vivo, the tissue-engineered cartilage implants exhibited strong repairing activity, maintained a chondrocyte-specific phenotype, and produced extracellular matrix components.

Conclusions: Focal gene delivery to aged articular chondrocytes exhibited strong repairing activity and may be therapeutically useful for articular cartilage regeneration.

Background

Osteoarthritis (OA), which is one of the most common, debilitating, and costly chronic disorders [1], is characterized by progressive degeneration or destruction of articular cartilage. Since the incidence of OA increases with age, the underlying mechanism of this disease may involve a loss of the capacity of chondrocytes to regenerate with age. In proliferative cells, telomeres from chromosomes gradually became shorter as a result of the DNA replication end problem. To prevent cessation of mitosis and premature cell death, telomerase is a ribonucleoprotein that is an enzyme which adds DNA sequence repeats (TTAGGG) to the 3' end of DNA strands in the telomere regions, which are found at the ends of chromosomes [2]. The telomerase allows for replacement of short bits of DNA known as telomeres, which are otherwise shortened when a cell divides via mitosis. In normal circumstances, without the presence of telomerase, if a cell divides recursively, at some point all the progeny will reach their Hayflick limit. With the presence of telomerase, each dividing cell can replace the lost bit of DNA, and any single cell can then divide unbounded. While this unbounded growth property has excited many researchers, caution is warranted in exploiting this property, as exactly this same unbounded growth is a crucial step in enabling cancerous growth. In immortal human tumor cells, the gene for the catalytic subunit of

* Correspondence: sato-m@is.icc.u-tokai.ac.jp
[1]Department of Orthopaedic Surgery, Surgical Science, Tokai University School of Medicine, 143 Shimokasuya, Isehara, Kanagawa 259-1193, Japan
Full list of author information is available at the end of the article

human telomerase reverse transcriptase (*hTERT*) is almost always derepressed [3]. Moreover, *hTERT* is not only an oncoprotein [2] but also a regulator of cellular differentiation [4,5].

As a result, immortalized human cells, such as epithelial and fibroblast cells [6] and chondrocytes [7,8], have been used as models of cellular aging. For example, Goldring [7] showed that primary human chondrocytes can be immortalized with retroviral transfection of 4 genes, including simian vacuolating virus 40 large T antigen and telomerase; however, stable transfection of *hTERT* in chondrocytes that are cultured in a monolayer allows maintenance of the proliferative capacity but not the chondrocyte phenotype. In contrast, Piera-Velazquez et al. [8] showed that exogenous expression of *hTERT* in chondrocytes that are cultured on polyhydroxyethylmethacrylate coated dishes increases their life span and maintains their chondrocyte phenotype. Thus, *hTERT* may extend the life span of chondrocytes.

Glucose-regulated protein 78 (GRP78) is a molecular chaperone in the endoplasmic reticulum (ER) that is induced by ER stress and prevents cell death as a result of homeostatic imbalance in the ER [9]. Although overexpression of *GRP78* can limit the damage from ER stress in normal tissues and organs, the natural induction of GRP78 in neoplastic cells also may promote cancer progression and drug resistance [10]. Since *GRP78* also is involved in the pathology of neurological diseases, such as Alzheimer's disease [11] and Parkinson's disease [12], GRP78 may have therapeutic cytoprotective effects to limit ER stress.

To determine whether *hTERT* and *GRP78* can prolong the life span of chondrocytes and stimulate cartilage regeneration, we transfected rabbit articular chondrocytes with these genes and redifferentiated chondrocytes in a 3-dimensional atelocollagen honeycomb-shaped scaffold with a membrane seal (ACHMS scaffold) [13]. We used this type of scaffold because it is biodegradable, supports the growth of high-density cell cultures, and maintains the phenotype of articular chondrocytes [14-16]. In addition, to investigate the clinical relevance of our model to OA, we investigated whether the effects of gene transfection depend on the age of the cartilage by analyzing the proliferation, gross morphology, cellular content of DNA and proteoglycans, and gene expression level of type II collagen in the transfected chondrocytes.

Methods

Preparation of chondrocytes

All animal experiments in this study approved by Research Support and Intellectual Property of the University of Tokyo were performed in accordance with their institutional guidelines for the care and use of laboratory animals.

Chondrocytes were prepared as described previously [14]. Briefly, articular cartilage tissue specimens were collected from the knee and shoulder joints of 4 young male (4 weeks old, 1 kg) and 8 old female (4 years old, 4.5 kg) Japanese white rabbits (Tokyo Laboratory Animals Science Co., Ltd., Tokyo, Japan). Each rabbit specimen was soaked and stored separately in basal medium (BM) containing Dulbecco's modified Eagle's medium (DMEM)/F12 (Gibco; Invitrogen, Carlsbad, CA, USA) supplemented with 10% heat-inactivated fetal bovine serum (FBS) (Gibco), 50 $\mu g \cdot mL^{-1}$ ascorbic acid (Wako Pure Chemical Industries, Osaka, Japan), and 1% Fungizone® antibiotic-antimycotic solution (10,000 $U \cdot mL^{-1}$ penicillin G, 10 $mg \cdot mL^{-1}$ streptomycin sulfate, and 25 $\mu g \cdot mL^{-1}$ amphotericin B; Gibco). When needed, cartilage samples were chopped into small pieces, and then digested for 1 h in DMEM/F12 containing 0.4% pronase E (Kaken Pharmaceutical, Tokyo, Japan), followed by digestion for 3 h at 37°C in DMEM/F12 containing 0.016% collagenase P (Roche Diagnostics, Mannheim, Germany). Subsequently, the digested samples were filtered with a cell strainer (BD Falcon™; BD Bioscience, Bedford, MA, USA) with a 100 μm pore size and the isolated cells were rinsed twice with chilled Dulbecco's calcium- and magnesium-free, phosphate-buffered saline (PBS) (Dainippon Pharmaceutical, Osaka, Japan). The number of viable chondrocytes was counted by using a Burker-Turk hemocytometer (Erma, Tokyo, Japan) with Trypan blue staining. Finally, the chondrocytes were seeded in 500 cm^2 square dishes (245 mm × 245 mm; Corning, Corning, NY, USA) at a density of 10,000 $cells \cdot cm^{-2}$ and cultured in BM with 10% FBS at 37°C in an incubator with 5% CO_2.

Retroviral transfection

Retroviral transfection of cultured chondrocytes was performed as described previously [17,18] with some modifications. First, DH5α *Escherichia coli* cells (from Hiroshima University Graduate School of Biomedical Sciences) were cultured overnight in lysogeny broth (LB) media [19] at 37°C. Subsequently, these cells were transfected with p*hTERT*-MSCV and p*GRP78*-MSCV plasmids to produce amphotropic viruses. The plasmids were amplified and purified by using an EndoFree Plasmid Maxi Kit (Qiagen, Tokyo, Japan). In addition, the sequence of all constructs was verified by DNA sequencing.

Next, these plasmids were used to produce retroviral constructs by using 2 different protocols. To produce the *hTERT* retroviral construct, full-length *hTERT* cDNA was polymerase chain reaction (PCR) amplified, and then cloned into the pMSCV-puro retroviral vector (Clontech, Mountain View, CA, USA). Subsequently, the cloned vector was transfected into the Retropack PT67 (Clontech) packaging cell line and the transfected cells were selected with puromycin (1.8 $\mu g \cdot mL^{-1}$) (Sigma

Aldrich, St. Louis, MO, USA) after 48 h. Two weeks after transfection, the surviving cells were trypsinized and allowed to continue to grow for up to 100 d. The culture supernatant from this cell line was collected and 0.45-μm filtered, and then polybrene (8 $\mu g \cdot mL^{-1}$) was added prior to transducing *hTERT* into young rabbit (YRA) and old rabbit (ORA) chondrocyte cultures.

Chondrocytes were cultured and plated 24 h before viral infection. Then, the packaged retrovirus was added to the culture media and incubated at 37°C in an incubator with 5% CO_2. The infected cells were selected with 0.5 $\mu g \cdot mL^{-1}$ of puromycin (Sigma Chemical) for 7-10 d prior to subsequent experiments.

To produce the *GRP78* retroviral construct, full-length *GRP78* cDNA was PCR amplified, and then inserted into the mouse stem cell virus (MSCV) packaging vector by using the Retrovirus Packaging Kit Ampho (TaKaRa Biotechnology, Shiga City, Japan) [20]. To produce *GRP78*-expressing retroviruses, 293 T cells (CRL-11268™, ATCC, Manassas, VA, USA) were seeded and maintained on 6-cm dishes at a density of 400,000 $cells \cdot cm^{-2}$ in DMEM containing 10% FBS for 24 h prior to transfection. Then, the culture medium was changed to the same medium. Subsequently, the 293 T cells were co-transfected with pGP (gag-pol) and pE-ampho (env) (TaKaRa Biotechnology) by using calcium phosphate transfection. Transfected cells were selected with 400 $\mu g \cdot mL^{-1}$ of hygromycin (Calbiochem, La Jolla, CA, USA) and 50 μg of mycophenolic acid (Sigma Aldrich). After 48 h, the culture medium, which contained the recombinant retroviruses, was 0.45-μm filtered, and then mixed with DMEM to infect YRA and ORA chondrocyte cultures.

Chondrocyte proliferation

Chondrocyte proliferation was measured by counting cell numbers at 100% confluence in serial passages. Briefly, nontransfected or *hTERT*/*GRP78*-transfected YRA and ORA chondrocytes, which were passaged once every 7-10 d, were detached by using 0.05% trypsin/ethylenediaminetetraacetic acid (EDTA; Gibco) for 20-30 min at 37°C and washed 3 times with PBS. An aliquot of the detached cells was used to count the mean number of cells from 6 dishes by using a Burker-Turk hemocytometer (Erma) with Trypan blue staining. The remaining cells were replated at a density of 5×10^3 $cells \cdot well^{-1}$.

Cell proliferation was expressed as the population doubling level (PDL). The PDL was calculated from log-phase growth curves by using the equation: $PDL = \log_{10}(N/N_0) \times 3.33$, where N_0 and N are the number of cells at the beginning and end of each experiment, respectively [21].

Preparation of the atelocollagen honeycomb-shaped scaffold with a membrane seal and 3-dimensional culture of chondrocytes

The ACHMS scaffold was prepared as described previously [13] by Koken (Tokyo, Japan). Briefly, nontransfected and *hTERT*/*GRP78*-transfected ORA chondrocytes were passaged twice, and then seeded at a density of 2×10^6 $cells \cdot scaffold^{-1}$ into a round ACHMS scaffold (diameter, 6 mm; thickness, 2 mm; average pore size, 200 μm) [13,14,22,23] in 48-well plates (Sumitomo Bakelite, Tokyo, Japan) by centrifuging at 45 *g* for 5 min. Then, these cell-seeded scaffolds were cultured in BM supplemented with 10% FBS at 37°C in an incubator with 5% CO_2 and 100% relative humidity for 14 d. These cultured chondrocytes were frozen in liquid nitrogen until needed for biochemical analyses and transplantation into an in vivo model of articular cartilage defects.

Measurement of DNA and glycosaminoglycans

The amount of DNA in the cultured ORA chondrocytes, which was used as a marker of cell proliferation, was measured by digesting cell-seeded scaffolds with papain, and then using a fluorimetric assay, as described previously [24]. Briefly, 15 μL of a papain digest was mixed with 300 μL of Hoechst 33258 solution (Polyscience, Warrington, PA, USA), and then a Titertek Multiscan Spectrofluorometer (Lab Systems, Helsinki, Finland) was used to measure the emission and excitation spectra at 456 nm and 365 nm, respectively. DNA concentrations were calculated from a standard curve of calf thymus DNA (Sigma).

The amount of glycosaminoglycans (GAGs) in the cultured chondrocytes, which was used as a marker of extracellular matrix (ECM) formation, was quantified by using 1,9-dimethylmethylene blue, as described previously [25]. Briefly, samples (140 μL) of each chondrocyte culture were mixed gently with an equal volume of 1,9-dimethylmethylene blue solution in a 96-well microtiter plate, and then the absorbance at 530 nm was measured with a Titertec multiscan spectrophotometer (Labsystem, Helsinki, Finland). The amount of GAGs was calculated from the absorbance values by using a standard curve of 0.625-20 $\mu g \cdot mL^{-1}$ shark chondroitin sulfate C (Seikagaku Kogyo Co, Tokyo, Japan).

Type II collagen mRNA expression

Frozen 3-dimensional cultures of ORA chondrocytes were pulverized with a Cryo-Press (Microtec Nition, Chiba, Japan) in liquid nitrogen. All oligonucleotide primer sets were designed on the basis of published mRNA sequences. The expected amplicon lengths ranged from 70 to 200 bp. Cloning of the entire coding region of type 2 collagen was performed by 5'- and 3'-rapid amplification of cDNA ends

using the following oligonucleotide primers: forward (5'-AACACTGCCAACGTCCAGAT-3'), reverse (5'-CTGC AGCACGGTATAGGTGA-3'). Real-time PCR was performed in a SmartCycler system (Cepheid, Sunnyvale, CA) with SYBR Green PCR Master Mix (Applied Biosystems, Foster City, CA) with 1 μL of cDNA template in a final volume of 25 μL. Amplification of cDNA was performed according to the following conditions: 95°C for 15 s and 60°C for 60 s for 35-45 amplification cycles. Changes in the fluorescence of SYBR Green were monitored after every cycle. Melting curve analysis was performed through a 0.5°C/s increase from 55 to 95°C with continuous fluorescence readings at the end of the cycles to ensure that single PCR products were obtained. All reactions were repeated in six separate PCR runs using RNA isolated from four sets of human samples. The results were evaluated by using SmartCycler software (Cepheid). Glyceraldehyde-3-phosphate dehydrogenase (GAPDH) primers were used to normalize the samples. To monitor crossover contaminations of PCR, RNase-free water (Qiagen, Valencia, CA) was used in the RNA extraction and as a negative control. To ensure the quality of data, a negative control was always included in each run.

Implantation of tissue-engineered cartilage produced from transfected aged chondrocytes

Twenty four old female Japanese white rabbits were divided into 4 groups (control 8w, 16w; hTERT + GRP78 8w, 16w) and anesthetized with intramuscular injections of 120 mg of ketamine (Daiichisankyo, Tokyo, Japan) and 9 mg of xylazine (Bayer HealthCare, Leverkusen, Germany). After creating a medial parapatellar incision in both legs, each patella was dislocated laterally and a cylindrical defect (diameter, 5 mm; depth, 3 mm) was created on the patellar groove of the femur in both legs by using a biopsy punch (Kai Industries, Seki, Japan) and a low-speed drill (Takagi, Niigata, Japan). The bottom of the subchondral bone also was shaved to a plane until marrow bleeding was observed. Then, ACHMS scaffolds that were seeded with either nontransfected or *hTERT*/*GRP78*-transfected ORA chondrocytes were allografted into these defects without any fixatives, such as fibrin glue. Postoperatively, all animals were allowed to walk freely in their cages without any splints.

Postoperative analyses

Eight and 16 weeks after implantation, rabbits were killed with an overdose of intravenous anesthesia, and then the distal parts of their femurs were harvested and observed with a light microscope. Subsequently, the femur samples were fixed in 10% buffered formalin for 7 d. Each specimen was decalcified with 10% EDTA in distilled water (pH 7.4) for 3 weeks, and then embedded in paraffin, cut into 6-μm-thick sagittal sections, deparaffinized, and stained with safranin O (Cartilage Staining Kit, Takara, Shiga, Japan). The histopathology of the OA cartilage samples (n = 24) were analyzed according to standard grading and staging of OA cartilage histopathology [26]. The OA score was calculated by the following formula: OA score = most degenerated site in the cartilage (grades 1-6, Table 1) × area of degeneration (stages 1-4) (Table 2).

Immunohistochemical staining for type II collagen was performed as described previously [14]. Briefly, after deparaffinization, the sections were pretreated with 0.1 mg·mL^{-1} of actinase E (Kaken Pharmaceutical) in PBS at 37°C for 30 min. Then, the sections were incubated with 10% pig serum at room temperature for 30 min to reduce nonspecific background staining. These pretreated sections were incubated overnight with 50 mg·mL^{-1} mouse anti-human type II collagen monoclonal antibody (Daiichi Fine Chemical, Toyama, Japan) in PBS containing 0.1% bovine serum albumin at 4°C. Next, the sections were incubated with biotinylated rabbit anti-mouse immunoglobulin (1:500 dilution; Dako, Carpinteria, CA, USA) for 30 min at room temperature, followed by peroxidase-conjugated streptavidin (1:500 dilution; Dako) for 30 min at room temperature. Finally, the sections were incubated with a solution of 20 mg of diaminobenzidine and 5 μL of hydrogen peroxide (30%) in 100 mL of PBS for 5 min at room temperature. Control sections were incubated with PBS without any antibodies and stained in a similar manner. These sections were analyzed by light microscopy.

Statistical analysis

One-way analysis of variance and Dunn's post hoc test was used to determine statistical significance ($P < 0.05$).

Results

Establishment of primary cultures of rabbit chondrocytes

During the first 3 weeks, YRA, ORA, ORA + *hTERT*, and ORA + *hTERT* + *GRP78* chondrocytes showed similar growth rates for 10 PDL (Figure 1). Later, ORA + *hTERT* and ORA + *hTERT* + *GRP78* chondrocytes proliferated more rapidly than the nontransfected chondrocytes. However, YRA + *hTERT* + *GRP78* chondrocytes had the fastest growth rate. In the control groups, YRA chondrocytes proliferated faster than ORA chondrocytes during the entire observation period, but their growth rate gradually decreased until they ceased at about 40 d and 60 d after the initiation of culture, respectively. Unlike control cells, which stopped proliferating after 10-20 PDL, ORA + *hTERT* and YRA + *hTERT* cells continued proliferating for about 35 and 50 PDL, respectively. These results showed that *hTERT* and *GRP78* increase the growth rate of transfected cells approximately 3-fold compared with nontransfected cells.

Table 1 OA cartilage histopathology grade assessment; grading methodology

Grade (key feature)	Associated criteria (tissue reaction)
Grade 1: surface intact	Matrix: superficial zone intact, oedema and/or superficial fibrillation (abrasion), focal superficial matrix condensation Cells: death, proliferation (clusters), hypertrophy, superficial zone Reaction must be more than superficial fibrillation only
Grade 2: surface discontinuity	As above + Matrix discontinuity at superficial zone (deep fibrillation) ± Cationic stain matrix depletion (Safranin O or Toluidine Blue) upper 1/3 of cartilage ± Focal perichondronal increased stain (mid zone) ± Disorientation of chondron columns Cells: death, proliferation (clusters), hypertrophy
Grade 3: vertical fissures (clefts)	As above Matrix vertical fissures into mid zone, branched fissures ± Cationic stain depletion (Safranin O or Toluidine Blue) into lower 2/3 of cartilage (deep zone) ± New collagen formation (polarized light microscopy, Picro Sirius Red stain) Cells: death, regeneration (clusters), hypertrophy, cartilage domains adjacent to fissures
Grade 4: erosion	Cartilage matrix loss: delamination of superficial layer, mid layer cyst formation Excavation: matrix loss superficial layer and mid zone
Grade 5: denudation	Surface: sclerotic bone or reparative tissue including fibrocartilage within denuded surface. Microfracture with repair limited to bone surface
Grade 6: deformation	Bone remodelling (more than osteophyte formation only). Includes: microfracturewith fibrocartilaginous and osseous repair extending above the previous surface

Grade = depth progression into cartilage

Characteristics of the 3-dimensional cultures of chondrocytes

The ACHMS scaffold supported a high density of ORA chondrocytes (2×10^6 cells·cm^{-2}) without any leakage of cells. During the 2-week culture, the chondrocytes in the scaffold retained their normal spherical shape (data not shown) and the resulting tissue-engineered cartilage maintained its shape and size in the ACHMS scaffold. The scaffolds were elastic and did not deform during culturing or collapse when handled with forceps.

Figure 2 shows macroscopic images of the cell-seeded scaffolds after culturing for 14 d. The scaffold that was seeded with *hTERT/GRP78*-transfected ORA chondrocytes had the highest cell density. In addition, the spaces between the atelocollagen matrix were filled and not visible along the edge of the ACHMS scaffold, which indicated that chondrocytes had proliferated throughout the scaffold during the cultivation period. In the scaffolds that were seeded with control cells, cell growth was sparse, and as a result, the spaces between the atelocollagen matrix remained mostly empty.

Glycosaminoglycan content of cell-seeded scaffolds

On day 14, the amount of GAG in cell-seeded scaffolds differed significantly between each group (Figure 3). Specifically, the total GAG content of scaffolds that were seeded with *hTERT/GRP78*-transfected ORA chondrocytes was higher than those that were seeded with *GRP78*- or *hTERT*-transfected cells. In addition, the GAG content of the scaffolds that were seeded with transfected ORA chondrocytes was higher than that in those that were seeded with nontransfected chondrocytes. These results suggested that transfected ORA chondrocytes were able to produce and accumulate significantly higher amounts of extracellular matrix components in the ACHMS scaffold than nontransfected chondrocytes.

Table 2 OA score; semi-quantitative method

Grade (key feature)	Stage % Involvement (surface, area, volume)			
	Stage 1 < 10%	Stage 2 10-25%	Stage 3 25-50%	Stage 4 > 50%
Grade 1(surface intact)	1	2	3	4
Grade 2 (surface discontinuity)	2	4	6	8
Grade 3 (vertical fissures, clefts)	3	6	9	12
Grade 4 (erosion)	4	8	12	16
Grade 5(denudation)	5	10	15	20
Grade 6(deformation)	6	12	18	24

Score = grade × stage

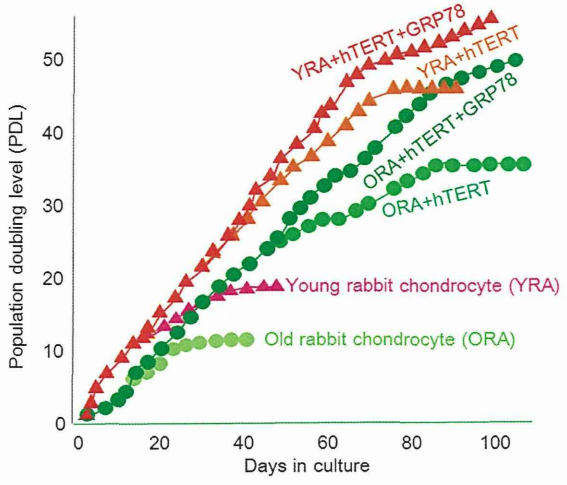

Figure 1 Effect of *hTERT* and *GRP78* on the proliferation of rabbit chondrocytes. Growth curves of cultures of nontransfected control chondrocytes from young and old rabbits (YRA and ORA, respectively) and *hTERT* (YRA + *hTERT* and ORA + *hTERT*) and *GRP78* (YRA + *hTERT* + *GRP78* and ORA + *hTERT* + *GRP78*)-transfected chondrocytes. The mean number of cells is shown on a $\log_{10}$ scale.

Type II collagen mRNA expression

As shown in Figure 4, the mRNA expression of type II collagen was observed in ORA, regardless of different gene transfection. Profiles of control, *GRP78*$^+$, *hTERT*$^+$, and *hTERT*$^+$/*GRP78*$^+$ cells were prepared to investigate expression of type II collagen. The mRNA expressions of *GRP78*$^+$, *hTERT*$^+$, and *hTERT*$^+$/*GRP78*$^+$ cells were significantly higher than that in control of non-transfective ORA. Chondrocytes are known to readily dedifferenciate in 2-dimensional culture. However, in this study, we used the primary culture of chondrocytes so that these chondrocytes retain their phenotype, which can be confirmed from type II collagen expression.

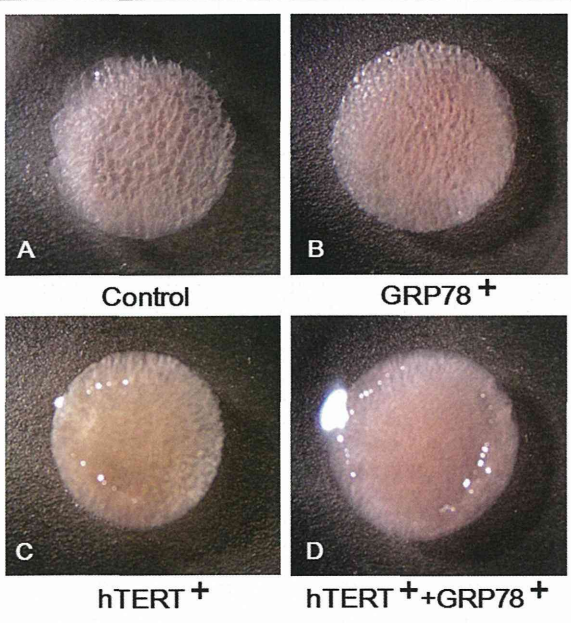

Figure 2 Macroscopic images of the cell-scaffold complex after 14 days of culture. Atelocollagen honeycomb-shaped scaffold with a membrane seal (ACHMS) scaffold complex seeded with nontransfected (A), *GRP78*-transfected (B), *hTERT*-transfected (C), or *hTERT*- and *GRP78*-transfected (D) ORA chondrocytes. Scale bar = 1.0 mm.

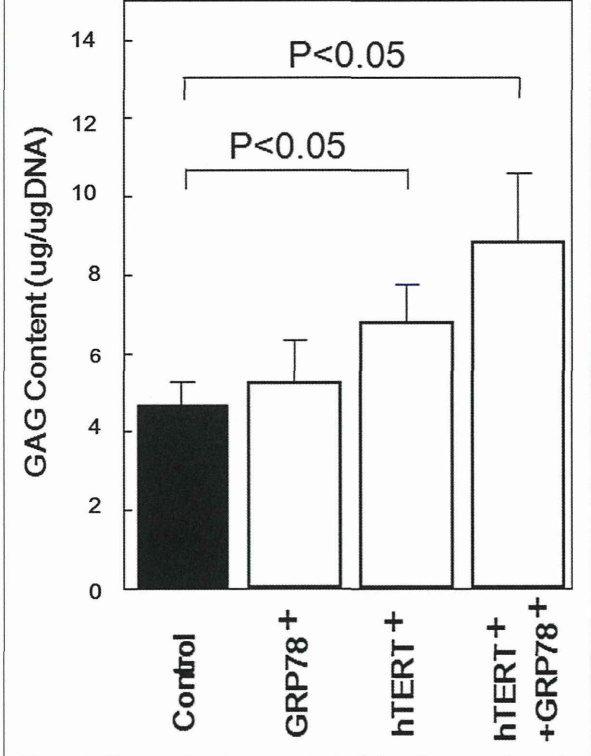

Figure 3 Glycosaminoglycan content of chondrocyte cultures in atelocollagen honeycomb-shaped scaffolds with a membrane seal. The glycosaminoglycan (GAG) content of nontransfected (black bars) or *hTERT*- or *GRP78*-transfected (white bars) ORA chondrocytes on the indicated days. Results are expressed as the mean (SD) of 6 independent measurements. *$P < 0.05$.

Macroscopic appearance of repaired osteochondral defects

The surgical implantation of tissue-engineered cartilage into osteochondral defects in the old rabbits was uneventful, and upon waking, all rabbits immediately resumed normal cage activity. At the time that they were killed, all rabbits exhibited unlimited passive range of motion in the knee joint.

Indeed, the osteochondral defects in old rabbits that were treated with tissue-engineered cartilage that was

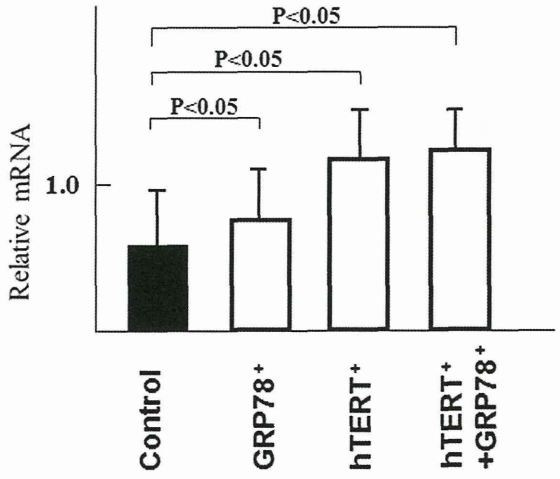

Figure 4 mRNA expression levels of type II collagen in transfected chondrocytes. The mRNA expression of type II collagen was observed in ORA, regardless of different gene transfection. Profiles of control, *GRP78*$^+$, *hTERT*$^+$, and *hTERT*$^+$/*GRP78*$^+$ cells were prepared to investigate expression of type II collagen. The mRNA expressions of *GRP78*$^+$, *hTERT*$^+$, and *hTERT*$^+$/*GRP78*$^+$ cells were significantly higher than that in control of non-transfective ORA. GAPDH was used as an internal control to normalize RNA levels.

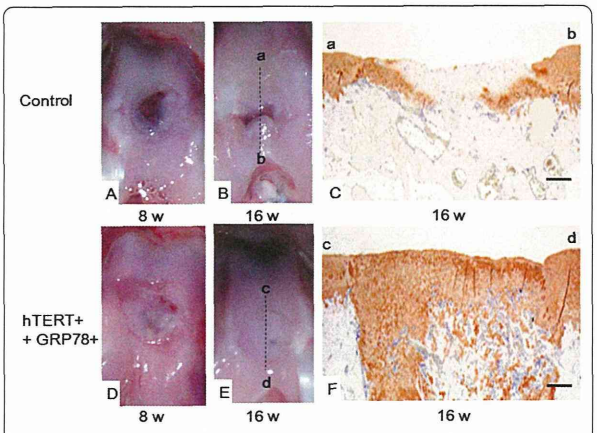

Figure 5 Macroscopic and immunostaining of regenerated cartilage after implantation. Postoperative appearance of repaired osteochondral defects in old rabbits implanted with scaffolds seeded with either nontransfected (top panels) or *hTERT*- and *GRP78*-transfected ORA chondrocytes (bottom panels) either 8 (A, D) or 16 (B, E) weeks after surgery. Immunostaining of type II collagen in tissue sections from rabbits implanted with scaffolds seeded with nontransfected (C) or *hTERT*- and *GRP78*-transfected (F) ORA chondrocytes. Each micrograph is representative of 8 tissue samples. Scale bar = 1.0 mm.

grown from *hTERT*- and *GRP78*-transfected ORA chondrocytes were filled with smooth tissue that resembled hyaline cartilage 16 weeks after surgery (Figure 5E) unlike the tissue-engineered cartilage that was grown from nontransfected ORA chondrocytes, which remained empty or were covered by fibrous tissue (Figure 5B). Although the control tissue-engineered cartilage showed some tissue repair along the borders of the defect, the color of the tissue was slightly different from that of the surrounding normal cartilage (Figure 5A, B).

Histological analysis of repaired osteochondral defects

No signs of arthritis, such as cartilage erosion or severe synovial proliferation, were observed in any surgically treated knee. In rabbits that were implanted with tissue-engineered cartilage grown from *hTERT*- and *GRP78*-transfected ORA chondrocytes, the immunohistochemical staining for type II collagen in the extracellular matrix in the scaffold was more intense and covered a larger area (Figure 5F) than those that were implanted with scaffolds that were grown from nontransfected ORA chondrocytes (Figure 5C). In addition, the tissue-engineered cartilage that was grown from transfected ORA chondrocytes was smooth and displayed good bonding with the host cartilage on both sides. In contrast, the tissue-engineered cartilage that was grown from nontransfected ORA chondrocytes had an irregular surface and was thinner than that grown from *hTERT*- and *GRP78*-transfected chondrocytes (Figure 5C).

As shown in Figure 6, the average OA scores were as follows: control 8w, 11.2 (2.5); 16w, 16.0 (3.2); hTERT + GRP78 8w, 17.3 (3.5); 16w, 21.00 (2.85). Statistically significant differences ($P < 0.05$) were observed between the transfected and nontransfected groups that were observed for the same period of time after implantation.

Discussion

Aging is the most important risk factor for both the initiation and progression of degenerative cartilage diseases. Osteoarthritic cartilage degeneration may be due to the loss of viable chondrocytes due to apoptosis or physical stress. This degeneration is likely to be closely related to age-related changes, since aging chondrocytes and articular cartilage matrix undergo senescence-like changes, which increase the susceptibility of cells to degenerative processes and environmental or physiological stresses [27]. As a result, chondrocytes from osteoarthritic patients might progress toward senescence more rapidly than those from normal individuals.

Aging chondrocytes also have important therapeutic ramifications. Recently, the treatment of articular cartilage defects have improved with the introduction of advanced tissue engineering techniques for autologous chondrocyte implantation (ACI) [28]. ACI requires cell expansion in culture to provide sufficient amounts of chondrocytes for reimplantation. However, like all mammalian cells, normal adult chondrocytes have a limited mitotic potential and eventually enter a state of senescence [29]. Moreover, the

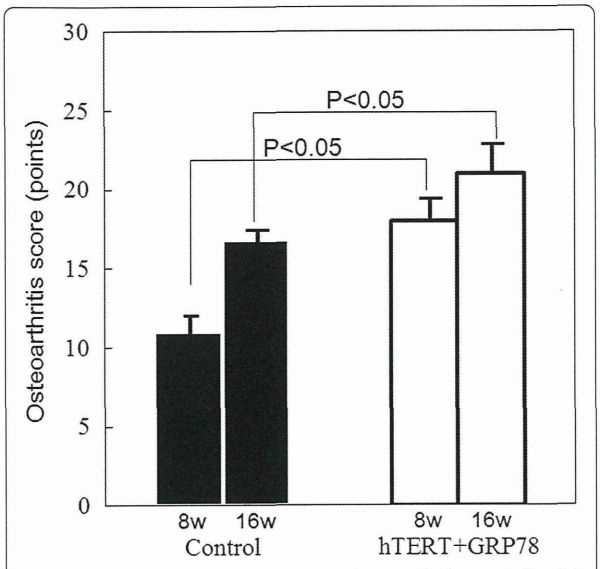

Figure 6 Osteoarthritis score. The histopathology of the OA cartilage samples from all 4 groups (n = 24) were analyzed according to standard grading and staging of OA cartilage histopathology. OA scores were calculated by using the following formula: OA score = most degenerated site in the cartilage (grades 1-6, Table 1) × area of degeneration (stages 1-4) (Table 2). Error bars indicate the standard deviation of each group. Statistically significant differences were observed between the control and hTERT + GRP78 groups 8 and 16 weeks after transplantation.

replicative life span of primary cells in culture are affected by the age of the donor, such that cells from older donors have a shorter life spans than those from younger donors [30]. For example, in monolayer cultures of aged human chondrocytes, serial passages rapidly results in loss of phenotypic stability and proliferative capacity [7]. Thus, to facilitate the therapeutic use of chondrocytes from older donors, a method is needed to prolong their replicative life span.

One possible method is transfection of *hTERT*, which can immortalize or prolong the life span of various human cells, such as muscle satellite cells [31,32], myoblasts [33,34], fibroblasts [6], and chondrocytes [7,8]. Since most immortalized cells maintain their phenotype and state of differentiation, *hTERT*-transfected cells are considered potential therapies for small-cell lung cancer [35] and for postnatal neovascularization in severe ischemic disease [36]. However, since chondrocytes uniquely maintain their phenotypes in 3-dimensional cultures [37], it is not known whether *hTERT*-immortalized chondrocytes maintain their state of differentiation.

Due to the aforementioned issues, in most cartilage tissue engineering studies, donor chondrocytes are usually from young animals. Our study is the first report that transfection of *hTERT* and *GRP78* can increase the replicative life span and therapeutic potential of tissue-engineered cartilage that is produced from ORA chondrocytes, which have a limited regenerative capacity. In addition, we used an ACHMS scaffold to maintain the phenotype of transfected chondrocytes, as indicated by the production of GAGs and type II collagen (Figures 3 and 4). These results are consistent with the findings of Piera-Velazquez et al. [8].

In this study, we overcame the limited lifespan of ORA chondrocytes by transfection with *hTERT* and increased their growth rate up to 3-fold by cotransfection with *GRP78* (Figure 1). Specifically, *hTERT/GRP78*-transfected ORA chondrocytes grew at a constant rate for more than 20 PDL, whereas nontransfected chondrocytes stopped dividing after much fewer PDL. However, we were not able to completely immortalize chondrocytes, even those from young rabbits (PDL < 50). Although the additional transfection of SV40-TAg or mutant Ras could immortalize these cells, we did not choose this option because the transfected cells may have become cancerous. As a result, we focused on the phenotypic stability of GRP78 and hTERT.

hTERT is a candidate gene for gene therapy of muscular dystrophy [31-34]. In contrast, *GRP78* may have therapeutic applications for neuropathological conditions, such as Alzheimer's disease, because it protects cells from ER stress [11,38-40]. ER stress can alter protein synthesis in cells [41]. One mechanism by which ER stress promotes apoptosis in cells is by driving the accumulation of structurally abnormal proteins [42], which are ordinarily repaired by ER chaperones to prevent age-related cell death. GRP78 is an example of a chaperone protein that regulates protein folding in the ER and thus contributes to cell survival [43]. Since the increase in the expression of GRP78 during cell culture may help protect cells from ER stress, overexpression of GRP78 also may protect cultured chondrocytes independent of hTERT.

Due to a lack of cages for mutant rabbits, we were not able to perform animal transplantation experiments with chondrocytes that were transfected with *hTERT* or *GRP78* alone. However, we believe that our in vitro and in vivo results from chondrocytes that were transfected with both *hTERT* and *GRP78* are sufficient to support our conclusions. In the future, we plan to perform more animal experiments to elucidate the effects of *GRP78*.

In conclusion, our results showed that tissue-engineered cartilage that was grown from implanted *in vivo* with *hTERT*- and *GRP78*-transfected ORA chondrocytes in ACHMS scaffolds can repair articular cartilage defects in vivo (Figure 5D, E, F). The *hTERT* and *GRP78*-transfected ORA exhibited proliferative and differentiation activity in articular cartilage defects, resulting in the formation of hyaline cartilage. This study also shows that ORA chondrocytes potentially produce hyaline cartilage after genetic treatment, similar to chondrocytes from young animals.

However, the mechanical strength of regenerated articular cartilage in large animals (*i.e.*, sheep or pigs) needs to be investigated.

Abbreviations

hTERT: Human telomerase reverse transcriptase; GRP78: Glucose-regulated protein 78; ER: Endoplasmic reticulum; ACHMS scaffold: Atelocollagen honeycomb-shaped scaffold with a membrane seal; OA: Osteoarthritis; BM: Basal medium; DMEM: Dulbecco's modified Eagle's medium; FBS: Fetal bovine serum; YRA: Young rabbit; ORA: Old rabbit; PDL: Population doubling level; RT-PCR: Reverse transcriptase-polymerase chain reaction; GAPDH: Gylceraldehyde-3-phosphate dehydrogenase; ACI: Autologous chondrocyte implantation; ECM: Extracellular matrix.

Acknowledgements

This work was supported by the Takeda Science Foundation, Grant of the New Energy and Industrial Technology Development Organization, and High-Tech Research Center Project 2004 for Private University. The funders had no role in study design, data collection and analysis, decision to publish, or preparation of the manuscript.

Author details

[1]Department of Orthopaedic Surgery, Surgical Science, Tokai University School of Medicine, 143 Shimokasuya, Isehara, Kanagawa 259-1193, Japan. [2]Biomedicinal Information Research Center, National Institute of Advanced Industrial Science and Technology (AIST), 2-42 Aomi, Koto-ku, Tokyo 135-0064, Japan. [3]Department of Biomedical Science & Technology, Institute of Biomedical Science & Technology (IBST), Konkuk University, 1 Hwang-dong, Gwangjin-gu, Seoul 143-701, Korea. [4]Department of Medical Engineering, National Defense Medical College, 3-2 Namiki, Tokorozawa, Saitama 359-8513, Japan. [5]Hiroshima University Graduate School of Biomedical Sciences, 1-2-3 Kasumi, Minami-ku, Hiroshima 734-8553, Japan.

Authors' contributions

MS, KS, MI, and TN conducted the experiments. MS, MI, NK, TK, HT, and GM analyzed the data. JIL performed the statistical analyses. MS, JIL, and JM wrote the manuscript. All authors read and approved the final manuscript.

Competing interests

The authors declare that they have no competing interests.

Received: 3 November 2011 Accepted: 2 April 2012
Published: 2 April 2012

References

1. Issa SN, Sharma L: **Epidemiology of osteoarthritis: an update.** *Curr Rheumatol Rep* 2006, **8**:7-15.
2. Harley CB: **Telomerase is not an oncogene.** *Oncogene* 2002, **21**:494-502.
3. Meyerson M, Counter CM, Eaton EN, Ellisen LW, Steiner P, Caddle SD, Ziaugra L, Beijersbergen RL, Davidoff MJ, Liu Q, Bacchetti S, Haber DA, Weinberg RA: **hEST2, the putative human telomerase catalytic subunit gene, is up-regulated in tumor cells and during immortalization.** *Cell* 1997, **90**:785-795.
4. Mattson MP, Fu W, Zhang P: **Emerging roles for telomerase in regulating cell differentiation and survival: a neuroscientist's perspective.** *Mech Ageing Dev* 2001, **122**:659-671.
5. Liu L, DiGirolamo CM, Navarro PA, Blasco MA, Keefe DL: **Telomerase deficiency impairs differentiation of mesenchymal stem cells.** *Exp Cell Res* 2004, **294**:1-8.
6. Hahn WC, Counter CM, Lundberg AS, Beijersbergen RL, Brooks MW, Weinberg RA: **Creation of human tumour cells with defined genetic elements.** *Nature* 1999, **400**:464-468.
7. Goldring MB: **Immortalization of human articular chondrocytes for generation of stable, differentiated cell lines.** *Methods Mol Med* 2004, **100**:23-36.
8. Piera-Velazquez S, Jimenez SA, Stokes D: **Increased life span of human osteoarthritic chondrocytes by exogenous expression of telomerase.** *Arthritis Rheum* 2002, **46**:683-693.
9. Reddy RK, Mao C, Baumeister P, Austin RC, Kaufman RJ, Lee AS: **Endoplasmic reticulum chaperone protein GRP78 protects cells from apoptosis induced by topoisomerase inhibitors: role of ATP binding site in suppression of caspase-7 activation.** *J Biol Chem* 2003, **278**:20915-20924.
10. Lee AS: **The glucose-regulated proteins: stress induction and clinical applications.** *Trends Biochem Sci* 2001, **26**:504-510.
11. Katayama T, Imaizumi K, Manabe T, Hitomi J, Kudo T, Tohyama M: **Induction of neuronal death by ER stress in Alzheimer's disease.** *J Chem Neuroanat* 2004, **28**:67-78.
12. Ryu EJ, Harding HP, Angelastro JM, Vitolo OV, Ron D, Greene LA: **Endoplasmic reticulum stress and the unfolded protein response in cellular models of Parkinson's disease.** *J Neurosci* 2002, **22**:10690-10698.
13. Sato M, Asazuma T, Ishihara M, Kikuchi T, Masuoka K, Ichimura S, Kikuchi M, Kurita A, Fujikawa K: **An atelocollagen honeycomb-shaped scaffold with a membrane seal (ACHMS-scaffold) for the culture of annulus fibrosus cells from an intervertebral disc.** *J Biomed Mater Res A* 2003, **64**:248-256.
14. Masuoka K, Asazuma T, Ishihara M, Sato M, Hattori H, Ishihara M, Yoshihara Y, Matsui T, Takase B, Kikuchi M, Nemoto K: **Tissue engineering of articular cartilage using an allograft of cultured chondrocytes in a membrane-sealed atelocollagen honeycomb-shaped scaffold (ACHMS scaffold).** *J Biomed Mater Res B Appl Biomater* 2005, **75**:177-184.
15. Ishihara M, Sato M, Sato S, Kikuchi T, Mochida J, Kikuchi M: **Usefulness of photoacoustic measurements for evaluation of biomechanical properties of tissue-engineered cartilage.** *Tissue Eng* 2005, **11**:1234-1243.
16. Glowacki J, Mizuno S: **Collagen scaffolds for tissue engineering.** *Biopolymers* 2008, **89**:338-344.
17. Pear WS, Nolan GP, Scott ML, Baltimore D: **Production of high-titer helper-free retroviruses by transient transfection.** *Proc Natl Acad Sci USA* 1993, **90**:8392-8396.
18. Fujita T, Otsuka-Tanaka Y, Tahara H, Ide T, Abiko Y, Mega J: **Establishment of immortalized clonal cells derived from periodontal ligament cells by induction of the hTERT gene.** *J Oral Sci* 2005, **47**:177-184.
19. Bertani G: **Lysogeny at mid-twentieth century: P1, P2, and other experimental systems.** *J Bacteriol* 2004, **186**:595-600.
20. Hawley RG, Lieu FH, Fong AZ, Hawley TS: **Versatile retroviral vectors for potential use in gene therapy.** *Gene Ther* 1994, **1**:136-138.
21. Cristofalo VJ, Allen RG, Pignolo RJ, Martin BG, Beck JC: **Relationship between donor age and the replicative lifespan of human cells in culture: a reevaluation.** *Proc Natl Acad Sci USA* 1998, **95**:10614-10619.
22. Itoh H, Aso Y, Furuse M, Noishiki Y, Miyata T: **A honeycomb collagen carrier for cell culture as a tissue engineering scaffold.** *Artif Organs* 2001, **25**:213-217.
23. Hattori H, Sato M, Masuoka K, Ishihara M, Kikuchi T, Matsui T, Takase B, Ishizuka T, Kikuchi M, Fujikawa K, Ishihara M: **Osteogenic potential of human adipose tissue-derived stromal cells as an alternative stem cell source.** *Cells Tissues Organs* 2004, **178**:2-12.
24. Kim YJ, Sah RL, Doong JY, Grodzinsky AJ: **Fluorometric assay of DNA in cartilage explants using Hoechst 33258.** *Anal Biochem* 1988, **174**:168-176.
25. Farndale RW, Buttle DJ, Barrett AJ: **Improved quantitation and discrimination of sulphated glycosaminoglycans by use of dimethylmethylene blue.** *Biochim Biophys Acta* 1986, **883**:173-177.
26. Pritzker KP, Gay S, Jimenez SA, Ostergaard K, Pelletier JP, Revell PA, Salter D, van den Berg WB: **Osteoarthritis cartilage histopathology: grading and staging.** *Osteoarthritis Cartilage* 2006, **14**:13-29.
27. Aigner T, Rose J, Martin J, Buckwalter J: **Aging theories of primary osteoarthritis: from epidemiology to molecular biology.** *Rejuvenation Res* 2004, **7**:134-145.
28. Brittberg M, Lindahl A, Nilsson A, Ohlsson C, Isaksson O, Peterson L: **Treatment of Deep Cartilage Defects in the Knee with Autologous Chondrocyte Transplantation.** *N Engl J Med* 1994, **331**:889-895.
29. Evans CH, Georgescu HI: **Observations on the senescence of cells derived from articular cartilage.** *Mech Ageing Dev* 1983, **22**:179-191.
30. Hayflick L: **The limited in vitro lifetime of human diploid cell strains.** *Exp Cell Res* 1965, **37**:614-636.
31. Cudre-Mauroux C, Occhiodoro T, Konig S, Salmon P, Bernheim L, Trono D: **Lentivector-mediated transfer of Bmi-1 and telomerase in muscle satellite cells yields a duchenne myoblast cell line with long-term genotypic and phenotypic stability.** *Hum Gene Ther* 2003, **14**:1525-1533.
32. Di Donna S, Renault V, Forestier C, Piron-Hamelin G, Thiesson D, Cooper RN, Ponsot E, Decary S, Amouri R, Hentati F, Butler-Browne GS, Mouly V:

Regenerative capacity of human satellite cells: the mitotic clock in cell transplantation. *Neurol Sci* 2000, **21(Suppl 5)**:S943-S951.
33. Seigneurin-Venin S, Bernard V, Moisset PA, Ouellette MM, Mouly V, Di Donna S, Wright WE, Tremblay JP: **Transplantation of normal and DMD myoblasts expressing the telomerase gene in SCID mice.** *Biochem Biophys Res Commun* 2000, **272**:362-369.
34. Seigneurin-Venin S, Bernard V, Tremblay JP: **Telomerase allows the immortalization of T antigen-positive DMD myoblasts: a new source of cells for gene transfer application.** *Gene Ther* 2000, **7**:619-623.
35. Song JS: **Adenovirus-mediated suicide SCLC gene therapy using the increased activity of the hTERT promoter by the MMRE and SV40 enhancer.** *Biosci Biotechnol Biochem* 2005, **69**:56-62.
36. Murasawa S, Llevadot J, Silver M, Isner JM, Losordo DW, Asahara T: **Constitutive human telomerase reverse transcripase expression enhances regenerative properties of endothelial progenitor cells.** *Circulation* 2002, **106**:1133-1139.
37. Watt FM: **Effect of seeding density on stability of the differentiated phenotype of pig articular chondrocytes in culture.** *J Cell Sci* 1988, **89(Pt 3)**:373-378.
38. Kudo T, Okumura M, Imaizumi K, Araki W, Morihara T, Tanimukai H, Kamagata E, Tabuchi N, Kimura R, Kanayama D, Fukumori A, Tagami S, Okochi M, Kubo M, Tanii H, Tohyama M, Tabira T, Takeda M: **Altered localization of amyloid precursor protein under endoplasmic reticulum stress.** *Biochem Biophys Res Commun* 2006, **344**:525-530.
39. Kudo T, Katayama T, Imaizumi K, Yasuda Y, Yatera M, Okochi M, Tohyama M, Takeda M: **The unfolded protein response is involved in the pathology of Alzheimer's disease.** *Ann N Y Acad Sci* 2002, **977**:349-355.
40. Yasuda Y, Kudo T, Katayama T, Imaizumi K, Yatera M, Okochi M, Yamamori H, Matsumoto N, Kida T, Fukumori A, Okumura M, Tohyama M, Takeda M: **FAD-linked presenilin-1 mutants impede translation regulation under ER stress.** *Biochem Biophys Res Commun* 2002, **296**:313-318.
41. Kozutsumi Y, Segal M, Normington K, Gething MJ, Sambrook J: **The presence of malfolded proteins in the endoplasmic reticulum signals the induction of glucose-regulated proteins.** *Nature* 1988, **332**:462-464.
42. Oyadomari S, Mori M: **Roles of CHOP/GADD153 in endoplasmic reticulum stress.** *Cell Death Differ* 2004, **11**:381-389.
43. Ni M, Lee AS: **ER chaperones in mammalian development and human diseases.** *FEBS Lett* 2007, **581**:3641-3651.

Pre-publication history
The pre-publication history for this paper can be accessed here:
http://www.biomedcentral.com/1471-2474/13/51/prepub

doi:10.1186/1471-2474-13-51
Cite this article as: Sato *et al.*: Human telomerase reverse transcriptase and glucose-regulated protein 78 increase the life span of articular chondrocytes and their repair potential. *BMC Musculoskeletal Disorders* 2012 **13**:51.

Journal of Gastroenterology and Hepatology

JGHF

doi:10.1111/jgh.12057

HEPATOLOGY

Characteristics of elderly hepatitis C virus-associated hepatocellular carcinoma patients

Takashi Kumada,* Hidenori Toyoda,* Seiki Kiriyama,* Makoto Tanikawa,* Yasuhiro Hisanaga,* Akira Kanamori,* Toshifumi Tada* and Junko Tanaka†

*Department of Gastroenterology, Ogaki Municipal Hospital, Ogaki, Gifu, and †Department of Epidemiology, Infectious Disease Control and Prevention, Graduate School of Biomedical Sciences, Hiroshima University, Hiroshima, Japan

Key words
alanine aminotransferase (ALT), alpha-fetoprotein (AFP), average integration value of ALT, elderly patient, hepatitis C virus (HCV), hepatocellular carcinoma (HCC), platelet count, propensity score.

Accepted for publication 14 October 2012.

Correspondence
Dr Takashi Kumada, Department of Gastroenterology, Ogaki Municipal Hospital, 4-86, Minaminokawa-cho, Ogaki, Gifu 503-8052, Japan. Email: hosp3@omh.ogaki.gifu.jp

Financial support: This work was supported by Health and Labour Sciences Research Grants (Research on Hepatitis) from the Ministry of Health, Labour and Welfare of Japan.

Declaration of conflict of interest: The authors report no conflicts of interest.

Abstract

Background and Aim: The average age of hepatitis C virus (HCV)-related hepatocellular carcinoma (HCC) patients has been rising in Japan. We evaluate characteristics of HCV-positive patients who develop HCC in older age to determine an optimal surveillance strategy.

Methods: A total of 323 patients with three or more years of follow-up before HCC diagnosis and 323 propensity-matched controls without HCC were studied. HCC patients were classified into four groups according to age at the time of HCC diagnosis: group A (≤ 60 years, $n = 36$), group B (61–70 years, $n = 115$), group C (71–80 years, $n = 143$), and group D (> 80 years, $n = 29$). Clinical and laboratory data were compared.

Results: Platelet counts were significantly higher in the older groups at HCC diagnosis ($P < 0.0001$). The rate of platelet counts decline was lower in older groups ($P = 0.0107$). The average integration value of serum alanine aminotransferase (ALT) in groups A, B, C, and D were 80.9 IU/L, 62.3 IU/L, 59.0 IU/L, and 44.9 IU/L, respectively ($P < 0.0001$). In older patients (≥ 65 years old), cirrhosis and average integration value of ALT were significantly associated with hepatocarcinogenesis, but platelet count was not.

Conclusion: Elderly HCV-positive patients (≥ 65 years old) with low ALT values developed HCC regardless of their platelet counts. These findings should be taken into account when designing the most suitable HCC surveillance protocol for this population.

Introduction

Hepatocellular carcinoma (HCC) is one of the most common malignancies, particularly in southern and eastern Asia. In Japan, HCC is the third leading cause of cancer death in men, behind lung and stomach cancer. In women, HCC is the fifth leading cause of cancer death during the past decade, behind colon, stomach, lung, and breast cancer.[1] Hepatitis C virus (HCV) infection accounts for approximately 75–80% of cases. Each year, HCC develops in 6–8% of patients with HCV-associated cirrhosis.[2]

In Japan, screening the blood supply for HCV, which commenced in November 1989 and began using second-generation enzyme immunoassays in February 1992, decreased the risk of post-transfusion hepatitis from more than 50% in the 1960s to virtually zero presently.[3] The age of Japanese patients diagnosed with HCC has been steadily increasing. Up to 1999, the majority of HCC mortalities occurred in patients under 69 years of age, but in 2000 more than half of HCC patients were over the age of 70.[1] This aging trend is also observed in HCV patients undergoing interferon-based therapy in Japan.[4] In contrast, HCV infection in the United States and other western countries is most prevalent among persons 30 to 50 years of age,[5] and the incidence of HCV-associated HCC is expected to rise. As a country with more experience with HCV-associated HCC, Japan's long-term experience can be helpful in planning strategies to contain HCV infection and to cope with its long-term sequelae worldwide.

The aim of this study is to evaluate characteristics of HCV-positive patients who develop HCC in older age and to determine an optimal surveillance strategy for these patients.

Materials and methods

Study population. This study cohort was comprised of 6740 consecutive HCV-positive patients (1019 patients with HCC and 5721 patients without HCC) referred to the Department of Gastroenterology at Ogaki Municipal Hospital from January 1990 to December 2006.

There were 323 patients who fulfilled the following inclusion criteria out of 1019 HCC patients: (i) detectable HCV-RNA for at least six months, (ii) no evidence of hepatitis B virus infection; (iii) other possible causes of chronic liver disease were ruled out

(no history of hepatotoxic drug use, and negative tests for autoimmune hepatitis, primary biliary cirrhosis, hemochromatosis, and Wilson's disease); (iv) a follow-up period of greater than three years before HCC diagnosis; (v) no interferon therapy within the last 12 months; and (vi) serum alanine aminotransferase (ALT) measurements taken more than twice yearly. The patients were classified into four groups according to age at the time of HCC diagnosis: group A (≤ 60 years, $n = 36$), group B (61–70 years, $n = 115$), group C (71–80 years, $n = 143$), and group D (> 80 years, $n = 29$).

Of the 5721 patients who have not developed HCC, 3275 patients fulfilled the same inclusion criteria. To reduce the confounding effects of covariates, we used propensity scores to match HCC patients with unique control patients based on age, sex, Child-Pugh classification at the start of follow-up, and follow-up duration. We were able to match 323 patients with HCC to 323 patients without HCC. The patients were classified into four groups according to age at the end of follow-up: group A' (≤ 60 years, $n = 30$), group B' (61–70 years, n = 114), group C' (71–80 years, $n = 136$), and group D' (> 80 years, $n = 43$).

The start of follow-up was defined as the date a patient first visited our hospital and ended on the date of HCC diagnosis for the HCC patients, or the date of the last visit at our hospital or December 31, 2010, whichever occurred earlier, in control patients.

Histological examinations were performed in 234 out of 646 patients. Cirrhosis was diagnosed pathologically in 120 patients. The remaining 412 patients were evaluated with ultrasonography (US) and biochemical tests.[6–8] Patients who did not satisfy the criteria for cirrhosis were classified as having chronic hepatitis for the purposes of this study. All together, 288 out of 646 patients were diagnosed with chronic hepatitis, and 358 were diagnosed with cirrhosis.

The study protocol was approved by the Ethics Committee at Ogaki Municipal Hospital in January 22, 2009 and complied with the Helsinki Declaration. Each patient provided written informed consent.

Laboratory test for liver disease and virologic markers. Platelet counts, prothrombin time, and serum levels of ALT, albumin, total bilirubin, alpha-fetoprotein (AFP), *lens culinaris* agglutinin–reactive fraction of AFP (AFP-L3%), and des-γ-carboxy prothrombin (DCP) were determined at the start of follow-up. ALT is expressed as an average integration value.[6] Serum AFP concentration was determined with a commercially available kit. AFP-L3 was measured by lectin-affinity electrophoresis and antibody-affinity blotting with the AFP Differentiation Kit L (Wako Pure Chemical Industries, Ltd, Osaka, Japan).[9] DCP was quantified with the Picolumi PIVKA-II kit (Eisai Co., Ltd, Tokyo, Japan).[10] HCV genotype was determined by PCR using genotype-specific primers, and HCV-RNA was quantified (before November 2007; COBAS Amplicor HCV monitor test and after December 2007; COBAS AmpliPrep/COBAS TaqMan HCV test, Roche Diagnostics K.K., Tokyo, Japan).

Alcohol exposure. Past alcohol exposure was estimated based on chart review of drinking patterns over five years. Patients were categorized as either "excessive" or "moderate" alcohol consumers. Excessive alcohol consumers drank over 50 g daily for five years.

Methods of follow-up. All patients received medical examinations at least every six months at our institution. Imaging studies, either US, computed tomography (CT), or magnetic resonance imaging (MRI), were performed at least every six months. When patients were considered to have developed cirrhosis by laboratory data or imaging findings, imaging was performed at three-month intervals.[11]

Diagnosis and treatment of HCC. The diagnosis of HCC was made based on either pathological or clinical and radiological criteria. Histological examination of resected hepatic tumors or US-guided needle biopsy specimens confirmed HCC in 165 patients (resected specimens: 111 patients; biopsy specimens: 54 patients). In the remaining 158 patients, the diagnosis of HCC was made using clinical criteria and imaging findings obtained from B-mode US, CT, MRI, and CT angiography.[12,13]

Tumor staging was performed according to the American Joint Committee on Cancer (AJCC) classification system.[14] In cases where pathologic evaluation was not available, vascular invasion was assessed by dynamic CT and angiography.

Treatment for each patient was individualized according to evidence-based clinical practice guidelines for HCC in Japan.[14] Hepatic resection was performed on 111 patients. Percutaneous ethanol injection therapy was performed in 16 patients. Radiofrequency ablation therapy was performed in 104 patients. Transcatheter arterial chemoembolization was performed in 62 patients. Thirty patients did not undergo treatment because of the patient's wishes or impaired liver function.

Statistical analyses. Statistical analysis was performed with the Statistical Program for Social Science (SPSS ver.18.0 for Windows; SPSS Japan Inc., Tokyo, Japan). Continuous variables are represented as medians (range). The non-parametric Jonckheere–Terpstra test was used to assess continuous variables. The Steel–Dwass or Shirley–Williams multiple comparisons method was applied if the Jonckheere–Terpstra test yielded significant results. The Cochran–Armitage test or the chi-square test was used to assess categorical variables. Actual survival was estimated using the Kaplan–Meier method,[15] and differences were tested with the log-rank test.[16] The Cox proportional hazards model and forward selection method were used to estimate the relative risk of HCC development associated with age, sex, cirrhosis, alcohol consumption, diabetes mellitus, effect of prior interferon therapy, platelet count, AFP at the start of follow-up, and average integration value of ALT, and the annual rate of platelet count decline. Statistical significance was set at $P < 0.05$.

Results

Clinical features at baseline. The clinical profiles of the HCC patients at the start of follow-up are shown in Table 1. There was a higher proportion of women diagnosed with HCC at a later age ($P = 0.0016$); the percentage of women in groups A, B, C, and

Table 1 Profile of HCV-infected HCC patients at the start of follow-up

	Group A ($n = 36$)	Group B ($n = 115$)	Group C ($n = 143$)	Group D ($n = 29$)	P
Sex (female/male)	5/31	43/72	63/80	15/14	0.0016
Age at the start of follow-up† (years)	49 (36–57)	59 (47–66)	66 (52–75)	74 (64–80)	< 0.0001
Duration of observation period until HCC diagnosis† (years)	6.4 (3.1–16.7)	6.9 (3.0–15.8)	8.0 (3.0–17.7)	9.3 (3.0–15.7)	0.0003
Alcohol consumption (≥ 50 g per day/< 50 g per day)	9/27	24/91	26/117	2/27	0.0873
History of blood transfusion (present/absent)	6/30	26/89	35/108	2/27	0.8247
Diabetes mellitus (present/absent)	24/12	40/75	51/92	5/24	0.0008
Prior interferon therapy (SVR/non-SVR/absent)	3/17/16	12/32/71	0/15/128	0/1/28	< 0.0001

†Expressed as median (range).
Group A, diagnosis of HCC at age ≤ 60 years; Group B, 61–70 years; Group C, 71–80 years; Group D, > 80 years.
HCC, hepatocellular carcinoma; HCV, hepatitis C virus; SVR, sustained virologic response.

Table 2 Profile of control patients with HCV infection at the start of follow-up

	Group A' ($n = 30$)	Group B' ($n = 114$)	Group C' ($n = 136$)	Group D' ($n = 43$)	P
Sex (female/male)	7/23	48/66	56/80	20/23	0.1175
Age at the start of follow-up† (years)	48 (40–56)	58 (48–67)	66 (54–75)	74 (65–82)	< 0.0001
Duration of observation period until the end of follow-up† (years)	7.0 (3.0–15.5)	7.8 (3.0–18.7)	8.5 (3.0–17.7)	8.5 (3.6–19.1)	0.0064
Alcohol consumption (≥ 50 g per day / < 50 g per day)	8/22	27/87	20/116	3/40	0.0630
History of blood transfusion (present/absent)	5/25	29/85	40/96	2/41	0.1939
Diabetes mellitus (present/absent)	7/23	38/76	47/89	12/31	0.0758
Prior interferon therapy (SVR/non-SVR/absent)	4/15/11	8/34/72	3/20/113	0/1/42	< 0.0001

†Expressed as median (range).
Group A', age ≤ 60 years at the end of follow-up; Group B', 61–70 years; Group C', 71–80 years; Group D', > 80 years.
HCV, hepatitis C virus; SVR, sustained virologic response.

D was 13.9, 37.4, 44.1, and 51.7, respectively. As the patient's age at HCC diagnosis increased, the patient's age at the start of follow-up and the duration of the observation period until HCC diagnosis increased ($P < 0.0001$ and $P = 0.0003$, respectively). Patients who received a diagnosis of HCC at a more advanced age have a significantly decreased incidence of diabetes mellitus and prior interferon therapy ($P = 0.0008$ and $P < 0.0001$, respectively). The clinical profiles of the control patients at the start of follow-up are shown in Table 2. The same tendency between HCC patients and control patients was observed.

Laboratory data of the HCC patients at the start of follow-up are shown in Table 3. Patients diagnosed with HCC at a more advanced age had lower baseline serum ALT and AFP levels ($P < 0.0001$ and $P = 0.0043$, respectively) and higher baseline platelet counts ($P = 0.0032$). In Table 4, the oldest group of control patients had lower baseline serum ALT and AFP levels ($P < 0.0001$ and $P = 0.0261$, respectively); however, no significant differences in baseline platelet count were observed.

The results of the Cox proportional hazards model and forward selection method to test factors associated with the age-related development of HCC to patient age at the start of follow-up are shown in Table 5. Ten covariates including age, sex, cirrhosis, alcohol consumption, diabetes mellitus, effect of prior interferon therapy, platelet count, baseline AFP, average integration value of ALT, and the annual rate of platelet count decline were studied. Age, cirrhosis, average integration value of ALT, platelet count, and AFP were significantly associated with hepatocarcinogenesis. However, only cirrhosis and average integration value of ALT were selected as factors significantly associated with hepatocarcinogenesis in patients ≥ 65 or 70 years old. Platelet count was not a significant factor.

Clinical features at the time of HCC diagnosis. Platelet counts at the time of HCC diagnosis in groups A, B, C, and group D were $72 \times 10^3/mm^3$ (40–192), $84 \times 10^3/mm^3$ (28–256), $99 \times 10^3/mm^3$ (31–355), and $119 \times 10^3/mm^3$ (58–232), respectively. There is a statistically significant trend toward higher platelet counts as the age at HCC diagnosis increases ($P < 0.0001$). In contrast, platelet counts at the end of follow-up in groups A', B', C', and D' were $194 \times 10^3/mm^3$ (44–543), $172 \times 10^3/mm^3$ (40–484), $177 \times 10^3/mm^3$ (21–415), and $193 \times 10^3/mm^3$ (52–429), respectively. There is no significant difference between the four groups of control patients ($P = 0.4772$). The annual rate of decline in platelet count, calculated as [platelet count at the start of the study period—platelet count at the time of HCC diagnosis]/duration of the observation period until the diagnosis of HCC, decreased significantly as the age at HCC diagnosis increased, and the annual rate of decline in platelet count, calculated as [platelet count at the start of study period—platelet count at the end of follow-up]/duration of observation period until the end of follow-up in control patients, did not increase significantly as the age at the end of follow-up increased (Fig. 1, $P = 0.0247$ and 0.1571, respectively). The annual rate of platelet count decline was

Table 3 Baseline laboratory data of HCV-infected HCC patients

	Group A ($n = 36$)	Group B ($n = 115$)	Group C ($n = 143$)	Group D ($n = 29$)	P
Platelet count† ($\times 10^3/mm^3$)	104 (34–249)	114 (29–253)	125 (44–307)	124 (70–201)	0.0032
Prothrombin time† (%)	87 (52–129)	88 (24–119)	85 (22–128)	86 (45–129)	0.6062
Total bilirubin† (mg/dL)	0.8 (0.3–1.8)	0.7 (0.2–4.7)	0.7 (0.3–6.7)	0.6 (0.2–1.3)	0.4583
ALT† (IU/L)	125 (24–361)	76 (18–387)	64 (8–154)	44 (17–221)	< 0.0001
Child-Pugh classification[17] (A or B/C)	33/3	103/12	130/13	24/5	0.5512
HCV genotype‡ (1/2)	26/6	66/24	75/29	15/6	0.4083
HCV viral concentration† (log copies/mL)	5.7 (2.7–8.0)	5.0 (2.0–8.0)	5.4 (2.0–6.9)	5.5 (3.0–7.0)	0.4952
AFP† (ng/mL)	13.5 (1.8–163.4)	8.4 (1.9–583.4)	7.2 (1.0–372.3)	4.8 (1.2–141.5)	0.0043
AFP-L3† (%)	0 (0–56.3)	0 (0–43.6)	0 (0–15.2)	0 (0–7.0)	1.0000
DCP† (mAU/mL)	19 (10–154)	19 (10–367)	17 (10–745)	15 (10–182)	0.0958
Cirrhosis (present/absent)	31/5	95/20	112/31	21/8	0.0903

†Expressed as median (range).
‡Data were unavailable for 76 patients.
AFP, alpha-fetoprotein; AFP-L3, *lens culinaris* agglutinin–reactive fraction of AFP; ALT, alanine aminotransferase; DCP, des-γ-carboxy prothrombin; Group A, diagnosis of HCC at age ≤ 60 years; Group B, 61–70 years; Group C, 71–80 years; Group D, > 80 years; HCC, hepatocellular carcinoma; HCV, hepatitis C virus.

Table 4 Baseline laboratory data of control patients with HCV infection

	Group A′ ($n = 30$)	Group B′ ($n = 114$)	Group C′ ($n = 136$)	Group D′ ($n = 43$)	P
Platelet count† ($\times 10^3/mm^3$)	204 (58–375)	180 (40–540)	187 (51–484)	196 (52–418)	0.4301
Prothrombin time† (%)	100 (52–138)	96 (38–153)	96 (48–144)	95 (47–145)	0.3435
Total bilirubin† (mg/dL)	0.5 (0.2–1.2)	0.4 (0.2–5.3)	0.4 (0.2–5.3)	0.3 (0.2–1.5)	0.6298
ALT† (IU/L)	53 (12–131)	46 (5–490)	35 (8–484)	22 (2–199)	< 0.0001
Child-Pugh classification[17] (A or B/C)	30/0	103/11	128/8	40/3	0.1088
HCV genotype‡ (1/2)	15/10	60/23	66/25	12/5	0.0869
HCV viral concentration† (log copies/mL)	5.9 (2.7–6.6)	5.7 (2.7–7.3)	5.8 (2.0–7.0)	5.1 (3.0–6.6)	0.1130
AFP† (ng/mL)	4.3 (0.8–156.3)	3.1 (0.8–170.3)	3.1 (0.8–219.2)	2.0 (0.8–29.2)	0.0261
AFP-L3† (%)	0 (0–26.9)	0 (0–34.2)	0 (0–41.4)	0 (0–5.2)	1.0000
DCP† (mAU/mL)	22 (10–122)	19 (10–487)	19 (10–503)	16 (10–30)	0.2549
Cirrhosis (present/absent)	5/25	35/79	48/88	11/32	0.1201

†expressed as median (range).
‡Data were unavailable for 107 patients.
AFP, alpha-fetoprotein; AFP-L3, *lens culinaris* agglutinin–reactive fraction of AFP; ALT, alanine aminotransferase; DCP, des-γ-carboxy prothrombin; Group A′, age ≤ 60 years at the end of follow-up; Group B′, 61–70 years; Group C′, 71–80 years; Group D′, > 80 years; HCV, hepatitis C virus.

Table 5 Factors associated with the development of HCC according to the age at start of follow-up in multivariate analysis

		All patients ($n = 646$) hazard ratio (95% CI)	≥ 60 years ($n = 428$) hazard ratio (95% CI)	≥ 65 years ($n = 255$) hazard ratio (95% CI)	≥ 70 years ($n = 92$) hazard ratio (95% CI)
Age (years)	≤ 60	1			
	> 60, ≤ 70	1.600 (1.240–2.064)			
	> 70	2.738 (1.858–4.036)			
Cirrhosis	Absent	1	1	1	1
	Present	2.165 (1.575–2.978)	2.269 (1.554–3.311)	2.734 (1.724–4.336)	2.962 (1.200–7.310)
Average integration value of ALT (IU/L)	≤ 20	1	1	1	1
	> 20, ≤ 40	4.239 (1.336–13.800)	4.885 (1.179–20.249)	5.243 (1.253–22.020)	12.162 (1.549–95.496)
	> 40, ≤ 60	5.518 (1.725–17.648)	6.661 (1.619–23.397)	6.739 (1.610–28.250)	6.797 (0.854–54.080)
	> 60, ≤ 80	7.182 (2.230–23.130)	9.362 (2.268–38.641)	12.265 (2.867–56.471)	11.183 (1.400–89.317)
	> 80	10.211 (3.175–33.031)	12.249 (2.494–50.884)	13.087 (2.962–57.815)	11.052 (0.964–126.671)
Platelet count ($\times 10^3/mm^3$)	≥ 150	1	1		
	< 150	1.644 (1.237–2.186)	1.728 (1.240–2.408)		
AFP* (ng/mL)	≤ 10	1			
	> 10, ≤ 20	1.406 (1.002–1.971)			
	> 20	1.609 (1.214–2.132)			

AFP, alpha-fetoprotein; ALT, alanine aminotransferase; CI, confidence interval; HCC, hepatocellular carcinoma.

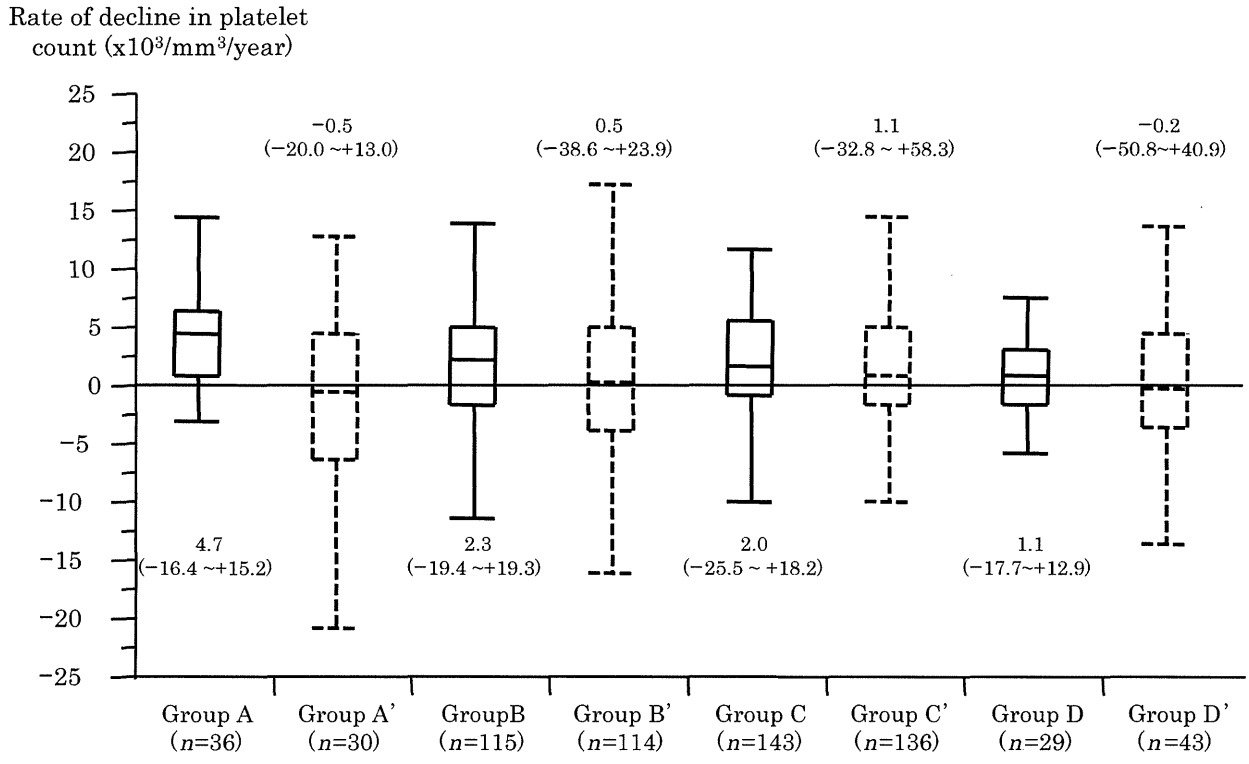

Figure 1 Rate of decline in platelet count prior to hepatocellular carcinoma (HCC) diagnosis in HCC patients and prior to the end of follow-up in control patients. The annual rate of platelet count decline in the period prior to HCC diagnosis was lower in the groups that were older at the time of HCC diagnosis. In control patients, there was no trend toward higher annual rates of platelet count decline in the period prior to the end of follow-up when the patients were classified by age ($P = 0.0247$ and 0.1571, respectively, Jonckheere-Terpstra Test). Group A, HCC diagnosed at age ≤ 60 years; group B, 61–70 years; group C, 71–80 years; group D, > 80 years. group A', control patients ≤ 60 years old at the end of follow-up; group B', 61–70 years; group C', 71–80 years; group D', > 80 years. The annual rate of platelet count decline was significantly lower in group A' than in group A ($P = 0.0039$); however, there were no significant differences when HCC patients in other age groups were compared to their respective matched controls.

lower in group A' than in group A ($P = 0.0039$), and there were no significant differences between group B and group B', group C and group C', and group D and group D'.

The average integration value of ALT in groups A, B, C, and D was 80.9 IU/L (25.3–179.3), 62.3 IU/L (14.5–167.9), 59.0 IU/L (9.9–134.1), and 44.9 IU/L (22.7–91.9), respectively. The average integration value of ALT was significantly lower in patients diagnosed with HCC at an older age (Fig. 2, $P < 0.0001$). There was a similar trend among control patients (Fig. 2, $P < 0.0001$). The average integration values of ALT in groups A', B', C', and D' were significantly lower than in groups A, B, C, and D, respectively ($P < 0.0001$).

Patient profiles at the time of HCC diagnosis are shown in Table 6. There were no significant differences in tumor characteristics and levels of tumor markers among the age groups. Fewer patients in Group D underwent hepatic resection ($P = 0.0293$).

Survival rates according to age at HCC diagnosis. Five and 10-year cumulative survival rates of groups A, B, C, and D were 44.2%, 58.2%, 44.3%, and 33.3% and 22.7%, 31.2%, 26.6%, and not available, respectively (Fig. 3). There were no significant differences in the cumulative survival rate among the four groups.

Discussion

In Japan, the average age of patients with chronic hepatitis, cirrhosis, or HCV-associated HCC is increasing. The number of deaths due to these diseases is also increasing. The age-specific prevalence of HCV seropositivity in the USA is about 30 years below that in Japan; thus, a majority of patients in the USA with chronic HCV infection will reach an advanced age in the near future.[3]

In our study, elderly HCC patients have high platelet counts and low ALT values. In addition, multivariate analysis using propensity-matched control patients revealed that the presence of cirrhosis and high ALT levels (> 20 IU/L) are significantly associated with the development of HCC. However, platelet count is not significantly associated with hepatocarcinogenesis in elderly HCV carriers (≥ 65 years). Physicians should be aware that patients aged 65 years or older could develop HCC regardless of their platelet count.

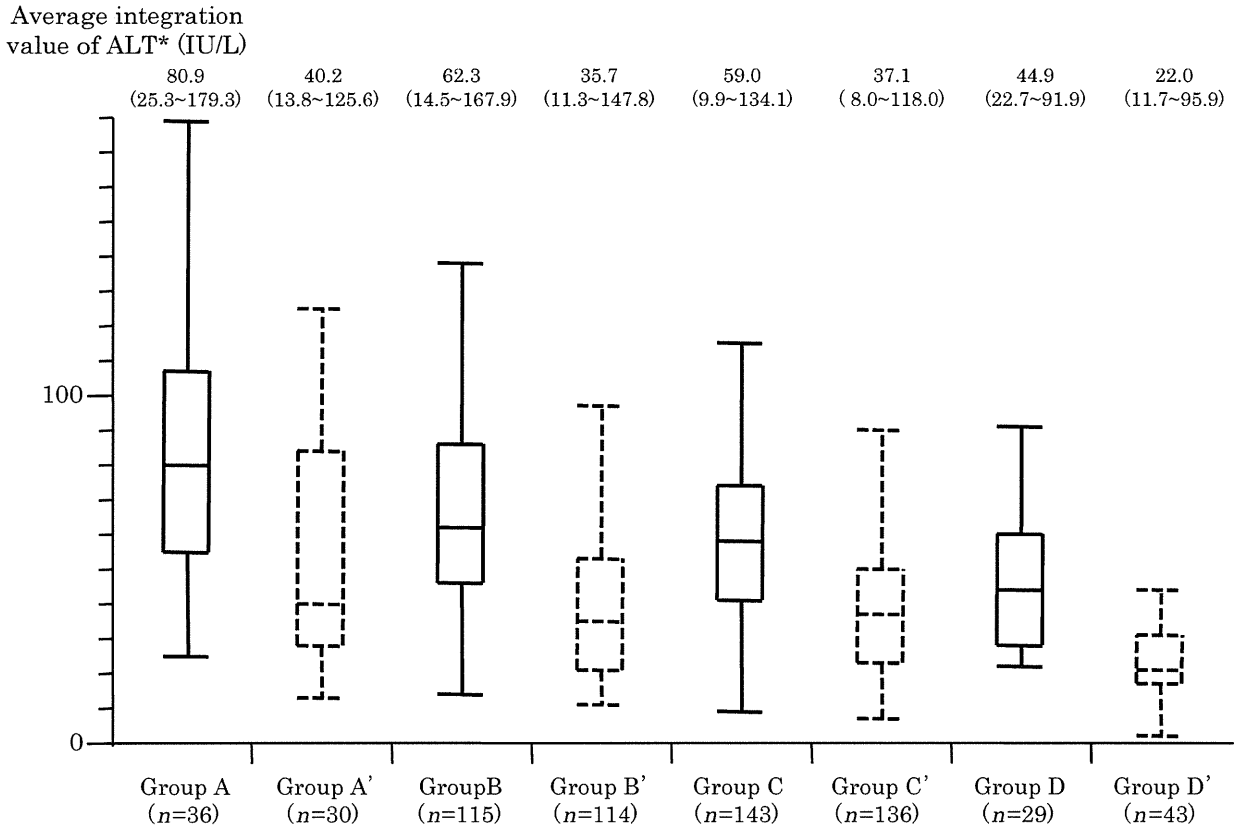

Figure 2 Average integration values of alanine aminotransferase (ALT) prior to HCC diagnosis in HCC patients and prior to the end of follow-up in control patients. Patients who were older at the time of HCC diagnosis had lower average integration values of ALT in the period prior to HCC diagnosis. In control patients, the average integration values of ALT in the period prior to the end of follow-up were lower in the groups that were older at the end of follow-up ($P < 0.0001$ and < 0.0001, respectively, Jonckheere-Terpstra Test). Average integration values of ALT in groups A', B', C', and D' were significantly lower than in groups A, B, C, and D, respectively ($P < 0.0001$).

Table 6 Profile of HCV-infected HCC patients at the time of HCC diagnosis

	Group A ($n = 36$)	Group B ($n = 115$)	Group C ($n = 143$)	Group D ($n = 29$)	*P*
AFP† (ng/mL)	23.9 (0.8–500)	19.8 (0.6–10500)	12.8 (0.8–12680)	17.8 (0.8–99720)	0.2347
AFP-L3† (%)	0 (0–89)	0 (0–87.2)	0 (0–81.0)	0 (0–40.7)	1.0000
DCP† (mAU/mL)	36 (10–36164)	35 (10–5941)	32 (10–50904)	24 (10–6229)	0.5650
Tumor size† (cm)	2.0 (0.8–10.0)	2.0 (0.3–8.8)	2.0 (0.6–11.4)	2.3 (1.0–9.0)	0.3754
Number of tumors†	1 (1–6)	1 (1–8)	1 (1–10)	1 (1–4)	1.0000
Portal thrombus (present/absent)	2/34	3/112	6/137	0/29	0.3293
Stage (1/2/3/4)	14/15/5/2	41/53/21/0	50/61/29/3	10/12/7/0	0.4957
Initial treatment (HR/PT/TACE/none)	9/18/4/5	47/44/16/8	51/47/33/12	4/11/9/5	0.0293

†Expressed as median (range).

AFP, α-fetoprotein; AFP-L3, *lens culinaris* agglutinin–reactive fraction of AFP; DCP, des-γ-carboxy prothrombin; Group A, diagnosis of HCC at age ≤ 60 years; Group B, 61–70 years; Group C, 71–80 years; Group D, > 80 years; HCC, hepatocellular carcinoma; HCV, hepatitis C virus; HR, hepatic resection; PT; percutaneous treatment including ethanol injection therapy, microwave coagulation therapy, and radiofrequency ablation therapy; TACE, transcatheter arterial chemoembolization.

The male-to-female ratio of HCC patients in Japan has decreased from 4.5 in 1984–1985 to 2.5 in 2002–2003.[1] It is well known that the mean age of female HCC patients with HCV infection is higher than that of males.[18,19] The increased proportion of female patients is considered a result of more older patients with HCV-related HCC. In our study, the proportion of female patients was the highest in group D. Further investigation of the role of sex in hepatocarcinogenesis is needed.

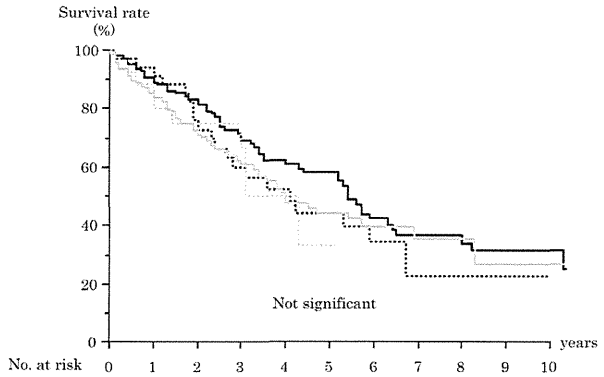

No. at risk	0	1	2	3	4	5	6	7	8	9	10
Group A	36	33	24	18	14	12	7	3	2	2	1
Group B	115	97	82	62	47	39	25	16	14	9	6
Group C	143	107	77	56	32	24	14	8	5	4	3
Group D	29	21	14	9	4	2	0	0	0	0	0

Figure 3 Cumulative survival rate of groups A, B, C, and D according to age at hepatocellular carcinoma (HCC) diagnosis. Kaplan-Meier curves showing the survival rate stratified by age at HCC diagnosis. There were no significant differences in the survival rate among the four groups. ——, A group (≤ 60 years, $n = 36$); ·····, B group (61–70 years, $n = 115$); ——, C group (71–80 years, $n = 143$); ·····, D group (> 80 years, $n = 29$).

We previously reported that the average integration value of ALT was associated with the cumulative incidence of hepatocarcinogenesis and that minimizing ALT is necessary for the prevention of hepatocarcinogenesis.[20] In addition, we demonstrated a 6.242-fold higher (95% confidence interval: 1.499–25.987) cumulative incidence of hepatocarcinogenesis in patients with average ALT integration values between 20 and 40 IU/L (within the current normal range) than in patients with 20 IU/L or below.[21] In this study, the average integration value of ALT significantly decreased as the age at HCC diagnosis increased. Especially in group D, the average integration value of ALT was 44.9 IU/L (range, 22.7–91.9 IU/L), which is near the upper limit of the conventional reference range of ALT (40 IU/L). There was the same tendency in control patients; however, average integration values of ALT were lower in control patients than HCC patients in each corresponding age group. These data suggest close surveillance for HCC is important even if older patients (≥ 65 years) have low ALT values.

It is likely that low platelet counts account for a large proportion of patients with cirrhosis, consistent with the theory that HCC develops in patients with progressive or advanced liver disease. Cirrhosis is an established risk factor for HCC in patients with HCV.[22,23] It is generally accepted that platelet count is a surrogate marker of liver fibrosis.[24,25] Platelet counts were highest in group D, both at the start of follow-up and at the time of HCC diagnosis. In contrast, there were no differences in platelet counts among control patients without HCC. It is particularly worth noting that group D had the smallest annual decline in platelet count, at levels comparable to the control patients. A previous report showed that the rate of progression of fibrosis to cirrhosis was accelerated by aging.[24] The precise mechanism of this discrepancy is uncertain. Probably, differences in patient selection might account for this discrepancy. We hypothesize that in our study, the increased rate of annual decline in platelet count may be linked to accelerated carcinogenesis occurring in the younger patients. Group D also had the lowest values of AFP, which is considered a marker of hepatic regeneration as well as a HCC tumor marker in viral hepatitis.[26] Taken together, this suggests a weaker inflammatory response in older patients. Further investigation is necessary.

Why do elderly patients progress to HCC even though liver function appears stable? Aging is associated with a number of events at the molecular, cellular, and physiological level that influence carcinogenesis and subsequent cancer growth.[22] Age may be considered as a progressive loss of stress tolerance due to declines in the functional reserve of multiple organ systems.[27] It has been hypothesized that age-associated declines in DNA repair[28] contribute to the development of HCC. The precise relationship between aging and hepatocarcinogenesis remains uncertain. Further assessment of the role of aging in the progression of HCV is needed.

We found no difference in tumor stage among the four groups. The younger groups A and B tended to receive curative therapy more often than the older groups C and D. However, there were no significant differences in survival. We hypothesize that this is due to the aggressive multiple treatments received by elderly patients with good liver function.

One limitation of our study is that histological confirmation was available in only 234 patients (36.2%). However, it is not practical to perform biopsies on all patients because of potential complications. Lu *et al.* reported that the best cutoff platelet count for the diagnosis of cirrhosis is 150×10^3 /mm^3.[29] Therefore, we employed platelet count as a surrogate marker of liver fibrosis in this study.

In conclusion, we demonstrated that elderly HCV-positive patients (≥ 65 years old) with low ALT values developed HCC regardless of their platelet counts. This finding should be taken into account when designating the most suitable HCC surveillance protocol. The optimal screening interval for HCV-infected patients aged 65 years older should be three to four months like cirrhotic patients even in the absence of cirrhosis.

References

1 Umemura T, Ichijo T, Yoshizawa K, Tanaka E, Kiyosawa K. Epidemiology of hepatocellular carcinoma in Japan. *J. Gastroenterol.* 2009; **44** (Suppl. 19): 102–7.
2 Kiyosawa K, Umemura T, Ichijo T *et al.* Hepatocellular carcinoma: recent trends in Japan. *Gastroenterology* 2004; **127** (Suppl. 1): S17–26.
3 Yoshizawa H. Hepatocellular carcinoma associated with hepatitis C virus infection in Japan: projection to other countries in the foreseeable future. *Oncology* 2002; **62** (Suppl. 1): 8–17.
4 Honda T, Katano Y, Urano F *et al.* Efficacy of ribavirin plus interferon-alpha in patients aged >or =60 years with chronic hepatitis C. *J. Gastroenterol. Hepatol.* 2007; **22**: 989–95.
5 El-Serag HB. Hepatocellular carcinoma and hepatitis C in the United States. *Hepatology* 2002; **36** (Suppl. 1): S74–83.
6 Shen L, Li JQ, Zeng MD, Lu LG, Fan ST, Bao H. Correlation between ultrasonographic and pathologic diagnosis of liver fibrosis due to chronic virus hepatitis. *World J. Gastroenterol.* 2006; **28**: 1292–5.
7 I Iacobellis A, Fusilli S, Mangia A *et al.* Ultrasonographic and biochemical parameters in the non-invasive evaluation of liver fibrosis in hepatitis C virus chronic hepatitis. *Aliment. Pharmacol. Ther.* 2005; **22**: 769–74.